Linköping University | Department of Electrical Engineering
Master's thesis, 30 ECTS | Electrical Engineering
2023 | LiTH-ISY-EX--23/5568--SE

Adaptive Rolling Radius Estimation

Adaptiv rullradie estimering

Rickard Wretlind
William Wärn

Supervisor : *Olov Holmer - ISY, Linköping University*
Examiner : *Jan Åslund - ISY, Linköping University*

External supervisor : *Kristoffer Lundahl - NIRA Dynamics AB*

LINKÖPING UNIVERSITY

Linköping University
SE–581 83 Linköping, Sweden
+46 13 28 10 00 , www.liu.se

Upphovsrätt

Copyright

Abstract

Tire tread health is essential for safe operation of a passenger vehicle. Worn out tires significantly increases the risk of traffic accidents and hydroplaning. This thesis investigates the possibility to detect tire tread wear by estimating the effective rolling radius of a tire. The effective rolling radius of a tire is affected by several different factors. As to not confuse change in external factors with actual tire tread wear, there is therefore a need to compensate the effective rolling radius to nominal conditions, to make sure that the change in compensated rolling radius is only due to the tire tread wear. This raises the questions: how can the effective rolling radius be estimated? Can it be compensated with respect to external factors?

The behavior of the tire changes between different tire models. This is because different models uses different materials, patterns, internal structure etc. This raises an additional question. Can a compensation model with the same parameter values be used in all vehicles of the same type no matter the tires of the vehicle, or is there a need for an adaptive compensation model that adapts the parameters to the current tire?

This thesis investigates how the estimation of the tires effective rolling radius can be improved by estimating the velocity using sensor fusion between GPS- and IMU-signals. This was done using an Extended Kalman Filter. Furthermore, this thesis proposes different ways of compensating a tires effective rolling radius with respect to external factors and compares these methods with each other to obtain the most efficient compensation method. After finding an appropriate compensation method, further investigations regarding the need of adaptivity between tires was performed to find out if the compensation factors can be used on the same vehicle model with different tire sets.

Ultimately, the investigations showed that the estimation of the effective rolling radius of a tire using sensor fusion was not fruitful due to limitations set by the IMU. If the vehicle had been equipped with a 6-axis IMU instead of a 3-axis IMU, this method might be feasible. The method that directly calculates the effective rolling radius from GPS-velocity and wheel speed gave a more accurate rolling radius signal. The compensation of the effective rolling radius can be achieved with respect to velocity, tire pressure and tire temperature. The most advantageous compensation method proposed in this thesis was a polynomial compensation model. Lastly, when investigating the need of adaptive compensation factors it was found that these compensation factors needs to be adaptive between tire sets.

Acknowledgments

We would like to express our deepest gratitude to our supervisor, Kristoffer Lundahl at NIRA Dynamics, who provided us with invaluable guidance and support throughout our thesis. Kristoffer's expertise, patience, and encouragement were instrumental in helping us navigate the research process and development of our thesis. We would also like to thank NIRA Dynamics for giving us the opportunity to study this subject with the guidance of their competent staff. Additionally we would like to thank our other colleagues at NIRA Dynamics for their help and support during the development process.

We would like to give a special thanks to Olov Holmer at Linköping University for his excellent guidance throughout the thesis. We would also like to thank Jan Åslund, our examiner for the thesis, for his deep wisdom within the field.

Additionally, we would like to thank our friends and families for their support and understanding throughout our studies. Thank you all for your help, encouragement, and support. Without your contributions, this thesis would not have been possible.

Linköping, May 2023
Rickard Wretlind and William Wärn

Nomenclature

ABBREVIATIONS

Abbreviation	Meaning
OEM	Original Equipment Manufacturer
FEM	Finite Element Method
GPS	Global Positioning System
WSS	Wheel Speed Sensor
IMU	Internal Measurement Unit
dTPMS	Direct Tire Pressure Monitoring System
NED	North-East-Down
EKF	Extended Kalman Filter
FL	Front Left Tire
FR	Front Right Tire
RL	Rear Left Tire
RR	Rear Right Tire
VW	Volkswagen

SYMBOLS

Notation	Description	Unit
r_e	Effective Rolling Radius of Wheel	mm
r_{fr}	Free-Rolling Radius of Wheel	mm
r_{ul}	Unloaded Radius of Wheel	mm
r_l	Loaded Radius of Wheel	mm
r_{nom}	Nominal Rolling Radius of Wheel	mm
r_{raw}	Raw Rolling Radius Signal	mm
r_{pc}	Pre-Compensated Rolling Radius of Wheel	mm
$r_{comp,l}$	Linear Compensated Radius of Wheel	mm
$r_{comp,vq}$	Velocity Quadratic Compensated Radius of Wheel	mm
$r_{comp,q}$	Quadratic Compensated Radius of Wheel	mm
$r_{comp,p}$	Pressure Compensated Radius of Wheel	mm
$r_{comp,V-Adaptive}$	Velocity Adaptive Compensated Radius of Wheel	mm
$\hat{r}_l$	Linear Rolling Radius Regression Model	mm
$\hat{r}_{vq}$	Velocity Quadratic Rolling Radius Regression Model	mm
$\hat{r}_q$	Quadratic Rolling Radius Regression Model	mm
$\hat{r}_{V-Adaptive}$	Velocity Adaptive Rolling Radius Regression Model	mm
v	Longitudinal Velocity	m/s
p	Pressure	kPa
l_{TD}	Tread Depth	mm
T	Temperature	$^\circ$C
Ω	Angular Velocity of the Wheel	rad/s
Ω_{WSS}	Wheel Speed Sensor Signal	rad/s
r_{raw}	Raw Rolling Radius	m
v_{GPS}	GPS velocity	m/s
q_v	Quadratic Speed Dependency Factor	mm/(km/h)^2
k_v	Speed Dependency Factor	mm/(km/h)
k_p	Pressure Dependency Factor	mm/kPa
k_{TD}	Tread Depth Dependency Factor	mm/mm
k_T	Temperature Dependency Factor	mm/$^\circ$C

Contents

List of Figures

List of Tables

1 Introduction

This master's thesis is done as a collaboration between Linköping University and NIRA Dynamics AB. This chapter introduces the thesis's background, purpose and formulates the problem. Furthermore, it includes delimitations to limit the scope of the thesis together with a section about previous related work within the area. Lastly the chapter present an outlined structure of the thesis.

1.1 Background

Tires are a vital component for the control of vehicles since the tires creates the contact points between the vehicle and the surface of the road and therefore creates the support for the car body. During driving, passenger vehicles are exposed to high forces and torques. All forces and torques, except for aerodynamical and gravitational forces, are transferred through the tires of the vehicle [1]. Abnormal tire forces on the vehicle can result in worse driving experience and an increased fuel consumption. Apart from these drawbacks, the likelihood of traffic accidents increase with decreasing tread depth [2]. This means that the properties of the tires are essential for the cars driving properties and safety.

One important aspect of the performance of a tire is its tread depth. In general, too shallow treads can lead to impaired grip between the tire and the road. Another common effect that can occur due to shallow treads is hydroplaning [3]. This issue has led to regulations regarding tread depth, in the European Union the legal limit for the tread depth is 1.6 mm [4]. Sweden has the same limit on summer tires, however, Sweden has additional requirements on winter tires, where the depth must be greater than or equal to 3.0 mm [5].

The tire health degradation is not evenly distributed between the four tires, but is rather dependent on several parameters such as: tire position, driver style, if the vehicle is front- or rear-wheel drive, and wheel alignment such as camber angle and toe angle [6]. It is the responsibility of the driver of a car to make sure that the tires follow regulation and have a tread depth greater than the legal limit. In modern vehicles there is no way for the vehicle to inform the driver that the tires are worn out, instead, the driver must manually check the tires. This check can be done by either measuring the tread depth or, if available, checking the tread wear indicators on the tires. This thesis aims at finding a model that can enable in-vehicle warnings about tire tread depths.

1.2 Problem Formulation

One method of estimating tire tread wear is by estimating and analyzing the effective rolling radius of the wheel. If one has a good estimate of the effective rolling radius one can calculate how much it has decreased over time. However, effective rolling radius depends on several factors. Some are determined by the tire itself, such as the type of structure (radial ply or bias ply), the wear of the tread, while others are determined by working conditions such as tire pressure, load, velocity, tire temperature, driving torque, braking torque and others [7]. The factors related to working conditions will be called external factors throughout this thesis. To enable tread wear estimation one needs to be able to compare the effective rolling radius in one time point with the effective rolling radius at another time point. To do this the effective rolling radius needs to be estimated under the same nominal conditions between time points. This is defined as the nominal rolling radius. Since the effective rolling radius depends on countless many factors, this nominal rolling radius is in practice unobtainable. A good estimate of this would be a signal that have nominal conditions for the major external factors. This will

be obtained by compensating the effective rolling radius. This compensated rolling radius can be used to compare with earlier measurements, without being affected by a change in the external factors that it is compensated for. Tire tread wear is a slow process and always decreasing, which means that the compensated rolling radius signal should decrease slowly and continuously over time. This means that the compensated rolling radius signal, should have minimal variance while decreasing steadily over time. This raises the questions: how can the effective rolling radius of a tire be estimated and how can it be compensated to nominal conditions? Another question is if the effective rolling radius dependency on the external factors is constant over time or if the dependency changes with time. If so, is there a need for a compensation model that is adaptive with regard to this?

There is a major difficulty with this task. That is, that when the tires on passenger vehicles are worn out, they are replaced with tires that might be different from the ones that came with the vehicle from the factory. Throughout this thesis, the assumption that the vehicle cannot determine what kind of tires a vehicle has at a given time, has been made. Even if the model would be restricted to only work on the tires that are approved by the OEM, this still results in several different tires. Each different variant of tire has different properties, such as different materials, tread patterns, original tread depth, width, height etc. This raises the question: is the effective rolling radius dependency on external factors different for different tire sets? Is there a need to take this into account when compensating the effective rolling radius for these factors?

Given the above, the following research questions are formulated:

- **RQ1** - Can a tire's rolling radius estimation be improved by estimating the velocity using sensor fusion?
- **RQ2** - How can the effective rolling radius of a tire be compensated with respect to external factors?
- **RQ3** - Is there a need for adaptive compensation factors between different tire sets?

1.3 Purpose and Goal

The purpose of this thesis is to investigate the possibility to develop an adaptive rolling radius compensation model to achieve a stable compensated rolling radius signal. This thesis has several goals. The first is to get a good estimate of the effective rolling radius of a tire. The second goal is to investigate if it is possible to compensate the effective rolling radius signal with regard to velocity, tire pressure and tire temperature. The third goal is to investigate if there is a need for adaptive compensation, i.e., is the compensation better if it is adapted to individual tire sets instead of using the same model on all different tires.

1.4 Delimitations

As mentioned above, the effective rolling radius of a tire depends on several factors. To enable tread wear estimation from the effective rolling radius, it needs to be compensated to nominal conditions for most of the external factors. This thesis will however only focus on velocity, tire pressure and tire temperature compensation. While the other external factors are compensated for using existing NIRA compensation models or are disregarded.

The purpose of this thesis is to enable tread wear estimation from a compensated rolling radius signal. However, this thesis is delimited to only focusing on obtaining the compensated rolling radius. The conversion from compensated rolling radius signal to tread wear is outside the scope of this thesis.

Furthermore, this thesis will exclusively consider front-wheel driven Volkswagen Passats. The vehicles used in this thesis have different tire models but they do have the same tire width of 215 mm. This means that this thesis will not investigate any effects of different tire widths. Additionally, this thesis will only be covering investigations on summer tires to avoid strange behaviors that could occur with winter tires. The thesis has also been limited to the sensors and data already available in these Volkswagen Passats.

A final product for tread wear estimation would need to be able to operate online in a vehicle. In-vehicle software usually has several computational limitations. This thesis aims to investigate if it is possible to compensate the effective rolling radius to nominal conditions, not how to do it online in a vehicle. Therefore, this investigation has been done with all available information with an offline method, even though an in-vehicle system would not be able to use this method. An offline method has the advantage of being able to train the model on the entire data set before using the model. This is not the case for an online model.

1.5 Related Work

Other authors have studied adaptive rolling radius estimation. In [8] a model to predict the tire tread wear of heavy-duty tires on a rubber-tired subway train, was developed. Their model was developed using FEM-analysis of a tire and a feedforward neural network. This model uses wheel travel speed, wheel rotational speed, vertical force, tire pressure and accelerometer data from inside the tire, as inputs to the model. Their model achieved an error of 0.21 mm. The major difference between their model and the one that will be developed in this thesis is that they had a specific tire for a specific vehicle, and since it is a commercial vehicle, they are certain that it will always use the same tire. For passenger cars this is not the case, if considering a country like, e.g. Sweden, at least two times a year each car owner has to change between summer and winter tires according to the law [5]. Tires are also replaced once they are worn out, and might not be replaced with the same tire variant. This model is applied to a rubber-tired subway train, a subway train tire is exposed to significantly different conditions than a tire on a passenger vehicle. According to [8] the force applied to each tire is 4150 kgf, significantly higher than the weight of an average car, this could lead to the tires being worn out faster compared to passenger cars. Another difference is that the train runs on a track, this means that it is exposed to a smoother surface with less or no bumps and potholes.

In [9] they studied the possibility to detect worn tires using different methods. They gathered data from a test vehicle on a test track where they drove the car under different conditions. Firstly, they drove it with four fresh tires and then drove it with one or two worn tires. They tried two different methods to detect the worn tire. First, they tried to detect the worn tire by comparing the rotational velocities between the different tires and the velocity of the vehicle, with the idea that the "odd one out" is worn out. However, they found that this method was not accurate enough to detect the worn tire. Instead, they compared slip with vehicle speed. They found that if no tire is worn out, the slip is mostly independent of speed, i.e., the slope in a slip-speed plot is close to 0. However, if one or two tires are worn out, they found that the slip increases with speed. This means that a worn tire can be detected by plotting slip against vehicle speed and calculate the slope. This work analyzes if a tire is worn compared to the other tires on the car, which makes their method in a sense binary, i.e., it detects if there is a worn tire or not. The worn tires used in testing had a tread depth of 4.9 mm, which is above the legal limit. This is the main difference between the method used in the paper and the purpose of this thesis. In a front-wheel drive vehicle, the front wheels are usually worn down quicker, meaning that the wear is in fact different. However, on a rear-wheel drive or all-wheel drive the wear might be more uniform, meaning that this method is not directly applicable. Therefore, in this thesis, a continuous update of the rolling radius measurement is needed to get the actual tread depth.

An approach to create a compensation algorithm to estimate the rolling radius was proposed in [10]. The paper focused on wheel radius analysis and how the distribution of the load in the vehicle can have an impact on the rolling radius on both the front and the rear tires. One factor that was addressed is the importance of the knowledge about the front and rear weight distribution. The proposed compensation algorithm makes use of the estimated offset in a longitudinal acceleration sensor.

Detecting tire wear using the effective rolling radius has been investigated in [11]. They proposed a model that estimates tire wear by keeping track of the unloaded tire radius of the wheels and how it changes over time. This unloaded tire radius was calculated using a formula depending on the effective rolling radius. The rolling radius was calculated using a Kalman filter on the GPS-velocity and wheel rotational speed. This model was validated on a car with a specific set of tires. The unloaded rolling radius model included three tuning parameters, if these parameters were car-tire specific or not was

not disclosed. It was also unclear how well it performed if the same model with the same parameters were to be used on the same car with a different set of tires. The paper also identified factors that affect the effective rolling radius. These include: tire wear, tire pressure, vehicle static loading and dynamic loading due to vehicle maneuvering, and type of tire (radial ply/bias ply). [12] further investigates how the effective rolling radius is dependent on inflation pressure and vertical loads.

Achieving an adaptive rolling radius model could be implemented by using state feedback with an observer. How to implement observers and observed state feedback is discussed in [13] and [14]. In [15] an observer-based parameter estimation scheme was developed with the purpose of estimating road gradient and vehicle weight using only the vehicle's velocity and driving torque. An alternate way of implementing state feedback is by using Kalman filters. This is discussed in [14] and [16]. Kalman filters are only applicable to linear systems. Nonlinear systems require other methods, one of which is Extended Kalman Filters. A method to estimate tire/road forces using an Extended Kalman Filter were investigated in [17]. Their aim was to use the tire/road forces to estimate the sideslip angle to prevent run-off-road accidents.

A method for rolling radius analysis using sensor fusion was proposed in [18]. The purpose of the analysis was to detect low tire pressure without tire pressure sensors. The paper proposed two approaches for this problem. The first approach uses two Kalman filters, one for each side of the vehicle, to detect change in rolling radius in relation to the other tire on that side using the wheel speed sensor. The second approach utilizes a Kalman filter that tries to detect relative change between tires on each axle using the yaw rate signal from a gyroscope. These two approaches are then combined to detect which tire has low tire pressure. Concerning Sensor Fusion, different algorithms in statistical sensor fusion were described in [19].

Previously investigated methods and approaches have been done within the field of both rolling radius estimation but also when it comes to rolling radius compensation. Related work regarding the rolling radius estimation have mainly be investigated on a given specific type of tire/tire sets. Other approaches have not been measuring the absolute rolling radius but rather exclusively comparing one or two tires to the others to find the "odd one out". Therefore, this literature is not directly applicable to the scope of this thesis. Methods for investigating rolling radius compensation approaches have mainly been based on how the vehicle is loaded, which is not quite the scope of this thesis, although some of the methods could be applicable to this thesis.

1.6 Thesis Outline

The thesis has the following outline.

- **Chapter 1** This chapter gives a background to the problem and formulates it.
- **Chapter 2** This chapter includes the theory used in the thesis.
- **Chapter 3** This chapter introduces the available test cases and the sensors used to gather the data.
- **Chapter 4** This chapter describes the rolling radius estimation method, result and discussion.
- **Chapter 5** This chapter presents the rolling radius compensation method, result and discussion.
- **Chapter 6** This chapter investigates the need for adaptivity between tire sets of the compensation model and includes the method, result and discussion.
- **Chapter 7** This chapter investigates the need for adaptivity over time of the compensation model and includes method, result and discussion.
- **Chapter 8** This chapter presents the conclusions of the thesis.
- **Chapter 9** This chapter presents and discusses further work that can be done within the area of adaptive rolling radius estimation.

2 Theory

This chapter presents the theory that is used in this thesis.

2.1 Rolling Radius

Rolling radius of a tire can be defined in several different ways. The different types of theoretical rolling radii covered in this thesis is the effective rolling radius, the free-rolling radius, the nominal rolling radius and the compensated rolling radius and these are described below. Furthermore, the calculated rolling radii from existing sensor signals, which are the raw rolling radius and the pre-compensated rolling radius, are described in Chapter 3.

2.1.1 Effective Rolling Radius

The effective rolling radius is the relationship between velocity and wheel speed [7]. It is defined as

$$r_e = \frac{v}{\Omega}. \tag{2.1}$$

where v is the velocity at the center of the wheel, Ω is the rotational velocity of the wheel and r_e is the effective rolling radius. As mentioned in Section 1.2 the effective rolling radius depends on several factors. Both tire specific factors such as the type of structure of the tire, the tread wear and tread pattern, and external factors such as load, velocity, tire pressure, tire temperature and applied torque. This means that the rolling radius can also be considered as a function of the above mentioned factors, since they will affect the behavior of v and Ω in (2.1), i.e., it can be described as

$$r_e = f_r(v, p, T, F_z, M, l_{TD}, \theta), \tag{2.2}$$

where p is the tire pressure, T is the tire temperature, F_z is the vertical load, M is the applied braking or driving torque and l_{TD} is the tread depth. Since the rolling radius depends on countless other minor factors these factors are collected in the variable θ. All of these variables depend on time.

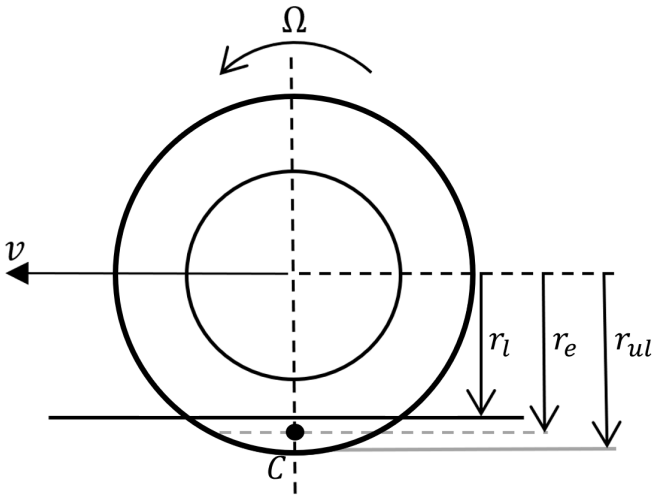

Figure 2.1: Illustration of the loaded wheel radius (r_l), the effective rolling radius (r_e) and the unloaded wheel radius (r_{ul}).

Figure 2.1 illustrates the difference between the different radii on a wheel. The unloaded wheel radius is the radius that the wheel would have if it was not in contact with the ground. The loaded wheel radius is the distance between the center of the wheel and the contact point with the ground. The effective rolling radius is the distance from the center of the wheel to the instantaneous center of rotation. The center of rotation is denoted as C in the figure.

While driving, the driven wheels will get a driving torque. This torque will lead to tire slip, which will make the wheel speed larger than if no slip occurred. This will push up the center of rotation and decrease the effective rolling radius, making it smaller than the loaded rolling radius [7]. If instead the vehicle is braking, the wheels will skid and the wheel speed is smaller than if no skid occurred [7]. This means that the center of rotation will be pushed down and the effective rolling radius will be greater than the unloaded radius.

2.1.2 Free-Rolling Radius

The free-rolling radius is the effective rolling radius when no torque is applied, meaning that no slip or skid is present. The free-rolling radius is usually somewhere between the loaded and unloaded rolling radius of the tire:

$$r_l < r_{fr} < r_{ul}. \tag{2.3}$$

The free-rolling radius can be described by the effective rolling radius function in (2.2) where the torque is fixed to the nominal value of 0. I.e.,

$$r_{fr} = f_r(v, p, T, F_z, M_0, l_{TD}, \theta), \tag{2.4}$$

where the subscript 0 indicates nominal conditions. In this case $M(t) = M_0$ for all t, where $M_0 = 0$ Nm.

2.1.3 Nominal Rolling Radius

The nominal rolling radius is in this thesis defined as the effective rolling radius that has been compensated to nominal conditions for all dependency factors except for tread depth. This is to remove any effects of change in working conditions on the effective rolling radius. Considering the function in (2.2), the nominal rolling radius can be described as

$$r_{nom} = f_r(v_0, p_0, T_0, F_{z_0}, M_0, l_{TD}, \theta_0), \tag{2.5}$$

where all variables are fixed to a nominal condition (described by index 0) except for the tread depth. This way, if one were to study the nominal rolling radius over time, it should in theory only change due to decrease in tread depth.

2.1.4 Compensated Rolling Radius

This thesis aims of obtaining a compensated rolling radius. This is defined as the effective rolling radius which has been compensated to get an estimate of the nominal rolling radius. So that it can be used to estimate tread wear. There is two major differences between the compensated rolling radius and the nominal rolling radius. The first difference is that the nominal rolling radius is nominal for all dependency factors except tread depth. This includes all minor factors that will not be studied in this thesis, that has been collected in a variable θ. Examples of such factors could be road surface conditions etc. The second difference is that the nominal rolling radius is "perfect" i.e., it has constant nominal conditions. The compensations that will be used in this thesis to achieve the compensated rolling radius can never be "perfect". The compensated rolling radius in this thesis shall be compensated for velocity, tire pressure, tire temperature, load and torque. The other factors that could affect the effective rolling radius, θ, are neglected. The nonlinearities that aren't handled by the compensations are also collected in, θ. The compensated rolling radius can be described as

$$r_{comp} \approx f_r(v_0, p_0, T_0, F_{z_0}, M_0, l_{TD}, \theta), \tag{2.6}$$

where r_{comp} is the compensated rolling radius.

2.2 Extended Kalman Filter

An Extended Kalman Filter or EKF, is a filter designed for nonlinear systems [19] on the form

$$X_{k+1} = f(X_k, u_k) + v_k, \tag{2.7}$$

$$Y_k = h(X_k, u_k) + e_k, \tag{2.8}$$

where X is the state vector, Y is the measurement vector, u_k is the input signal, v_k is process noise and e_k is measurement noise. This model assumes additive noise. f is the state transition function and h is the measurement function. The noise variables has corresponding covariance matrices; Q for the process noise and R for the measurement noise. There is also a covariance matrix P that describes the uncertainty of the state variable X. There are both first and second order EKF:s but this thesis will only use a first order EKF. The EKF in this thesis will not include an input signal u_k. A first order EKF utilizes a first order Taylor expansion of the nonlinear functions, to approximate them as linear functions. This allows for a filter that uses a similar method as a regular linear Kalman filter.

2.2.1 Algorithm

The EKF algorithm is divided into two steps, a measurement update and a time update [19]. The measurement update starts with calculating the variable S_k which is defined as

$$S_k = R_k + h'(\hat{X}_{k|k-1})P_{k|k-1}(h'(\hat{X}_{k|k-1}))^T, \tag{2.9}$$

where h' is the jacobian of the measurement function. The subscript k corresponds to an arbitrary time point k and $k|k-1$ corresponds to the time point k given knowledge (measurements) up to the previous time point $k-1$. Next comes the variable K_k which is calculated by

$$K_k = P_{k|k-1}(h'(\hat{X}_{k|k-1}))^T S_k^{-1}. \tag{2.10}$$

The actual measurement update is calculated as

$$\hat{X}_{k|k} = \hat{X}_{k|k-1} + K_k(Y_k - h(\hat{X}_{k|k-1})). \tag{2.11}$$

Finally the covariance matrix P is updated as

$$P_{k|k} = P_{k|k-1} - P_{k|k-1}(h'(\hat{X}_{k|k-1}))^T S_k^{-1} h'(\hat{X}_{k|k-1})P_{k|k-1}. \tag{2.12}$$

The measurement update consists of firstly updating the state estimate with the state transistion function

$$\hat{X}_{k+1|k} = f(\hat{X}_{k|k}), \tag{2.13}$$

and then updating the covariance matrix

$$P_{k+1|k} = Q_k + f'(\hat{X}_{k|k})P_{k|k}(f'(\hat{X}_{k|k}))^T, \tag{2.14}$$

where f' is the jacobian of the state transition function. The subscript $k+1|k$ means that it is an estimate of the value of the variable for the time point $k+1$ given measurements up to time point k.

2.3 Linear Least Squares Regression

Linear least squares regression is a method to find the coefficients of a polynomial model that fits any arbitrary data set the "best". This is done by using an error function and finding the solution that minimizes the error squared [20]. The error is defined as

$$e_i = y_i - \hat{y}_i, \tag{2.15}$$

where y_i is the measured value of the output and $\hat{y}_i$ is the output estimated from the regression model. Least squares regression solves the optimization problem that minimizes the square of the model error. The error is squared to remove the sign of the error while keeping it continuous and differentiable. The optimization problem is defined as

$$\min_K \sum_{i=1}^{n} (e_i)^2, \tag{2.16}$$

where K is the coefficients of the regression model.

Least squares regression can be done by using matrix notation. If one wants to fit data to the affine model

$$k_1 \cdot x + k_2 \cdot z + m = \hat{y}, \tag{2.17}$$

it can be rewritten on matrix form as

$$a \cdot K = b, \tag{2.18}$$

where $b = y$, $a = [x, z, 1]$ and $K = [k_1, k_2, m]^T$. If one applies this model to a dataset of measurements then one gets the matrix of input data

$$A = \begin{bmatrix} x_1 & z_1 & 1 \\ x_2 & z_2 & 1 \\ x_3 & z_3 & 1 \\ \vdots & \vdots & \vdots \end{bmatrix}, \tag{2.19}$$

and the vector of output values

$$B = \begin{bmatrix} y_1 \\ y_2 \\ y_3 \\ \vdots \end{bmatrix}. \tag{2.20}$$

Then the least squares is the model that finds the coefficents K, that fits the data best with regards to the error distance squared. This is done by solving the equation

$$A \cdot K = B, \tag{2.21}$$

by

$$A^T \cdot A \cdot K = A^T \cdot B, \tag{2.22}$$

and

$$K = (A^T \cdot A)^{-1} A^T \cdot B. \tag{2.23}$$

The expression $(A^T \cdot A)^{-1} A^T$ is simply the psuedo inverse of the matrix A. The equation can therefore simply be written as

$$K = A^{\dagger} B. \tag{2.24}$$

The psuedoinverse can be applied by using the \operator in Matlab.

2.3.1 Least Squares Drawbacks

The least squares regression method has a drawback in the fact that the error distance is squared. This makes it sensitive to outliers in the dataset. One method to solve this is to remove "obvious" outliers. Another way is by having large amounts of data, so that there might be a more even distribution of outliers both above and below the ground truth.

2.3.2 R Squared

R Squared (R^2) is a measure of the ratio between the variance explained by the model and the total variance of the signal [20]. A low R^2 value means that a lot of the noise in the signal is not explained by the regression model. It is defined as

$$R^2 = \frac{RegSS}{TSS}, \tag{2.25}$$

where $RegSS$ is the sum of squares from the regression, which is defined as

$$RegSS = \Sigma_i(\hat{y}_i - \bar{y})^2, \tag{2.26}$$

where $\hat{y}_i$ is the modelled y-value at x_i, y_i is the measurred y-value at x_i and $\bar{y}$ is the average y-value of the data set. TSS is the total sum of squares, which is defined as

$$TSS = \Sigma_i(y_i - \bar{y})^2. \tag{2.27}$$

3 Test Cases and Data Measuring

This chapter includes all the information regarding the test cases and the data measuring used throughout this thesis.

3.1 Test Data

The models developed in this thesis have been tested on data gathered from real vehicles on real roads. However, having data gathered from cars on the roads means that there is no additional information about the circumstances of the test case. E.g., there is no ground truth velocity, there is no knowledge about which roads it drove on. Since tread wear is a slow process the test data needs to have been collected over long periods of time. This thesis had access to four long term test cases. All are front-wheel driven Volkswagen Passats with different types of summer tires. Two of the test cases are on the same car individual: Test Case 2 and Test Case 3.

Table 3.1: This table displays the different test cases that are used during this thesis.

Test Case	Car Type	Tire Type	Duration [s]	Distance [km]
Test Case 1	VW Passat	Kleber Dynaxer HP4 215/60-16	2,425,849	27,169
Test Case 2	VW Passat	Hankook Ventus Prime 3 K125	1,847,793	20,203
Test Case 3	VW Passat	ContiEcoContact 215/60-16	2,425,849	27,169
Test Case 4	VW Passat	Michelin Primacy 4 215/60-16	2,444,988	36,010

The models in this thesis were mainly developed on one test case and then validated on several test cases. The main test case used is called Test Case 4, it is approximately 694 h long and covers a distance of 36,010 km. The measured tread wear for all test cases are shown in Table 3.2. These values are collected by measuring the tread depth before and after the whole test case and calculating the difference.

Table 3.2: The measured tread wear for all test cases.

Test Case	FL [mm]	FR [mm]	RL [mm]	RR [mm]
Test Case 1	4.14	3.91	3.11	3.05
Test Case 2	4.94	4.54	1.23	1.54
Test Case 3	4.11	3.48	0.96	1.10
Test Case 4	3.70	3.52	1.40	1.67

The tire pressure has a large impact on the effective rolling radius of a tire and can vary a lot over time due to several factors. One factor is tire permeation which all tires suffer from. It is a process where the air molecules diffuses, or leaks, through the rubber of the tire. Different tires suffer from different amounts of permeation, but all tires have some diffusion. Tires can also suffer from leaking valves which leads to an even greater pressure drop over time. The tires can also be manually inflated or deflated. Furthermore, tire pressure increases with temperature. All of this leads to the fact that the tire pressure signal can vary greatly over time and between different tire sets.

In Figure 3.1 one can see that the tire pressures for Test Case 1 are rather stable over time. There seems to have been some issue with the signal in the initial part of the test case. This will however not affect the compensations in Chapter 5, because they will be performed after the initial 500,000 s to not

be affected by the initial tire growth, see Section 5.1.3. For Test Case 2 there is significant pressure loss over time, see Figure 3.2. There also seems to be some tire inflation on the front tires at 1,500,000 s. For Test Case 3 there is low diffusion making the pressure signal stable over time, see Figure 3.3. There is however a manual tire deflation about halfway through the test case. The tire pressures for Test Case 4 is presented in Figure 3.4. It has an overall pressure loss over time.

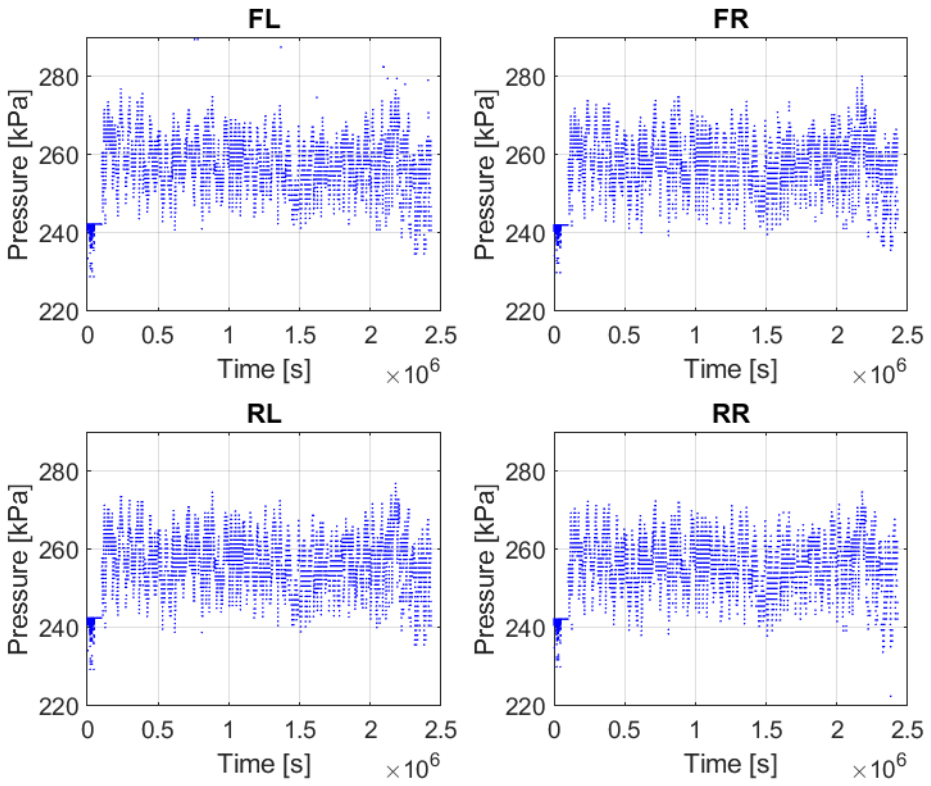

Figure 3.1: This figure shows the pressure signal for all tires for Test Case 1. This signal has been enhanced using the method described in Section 5.1.2.

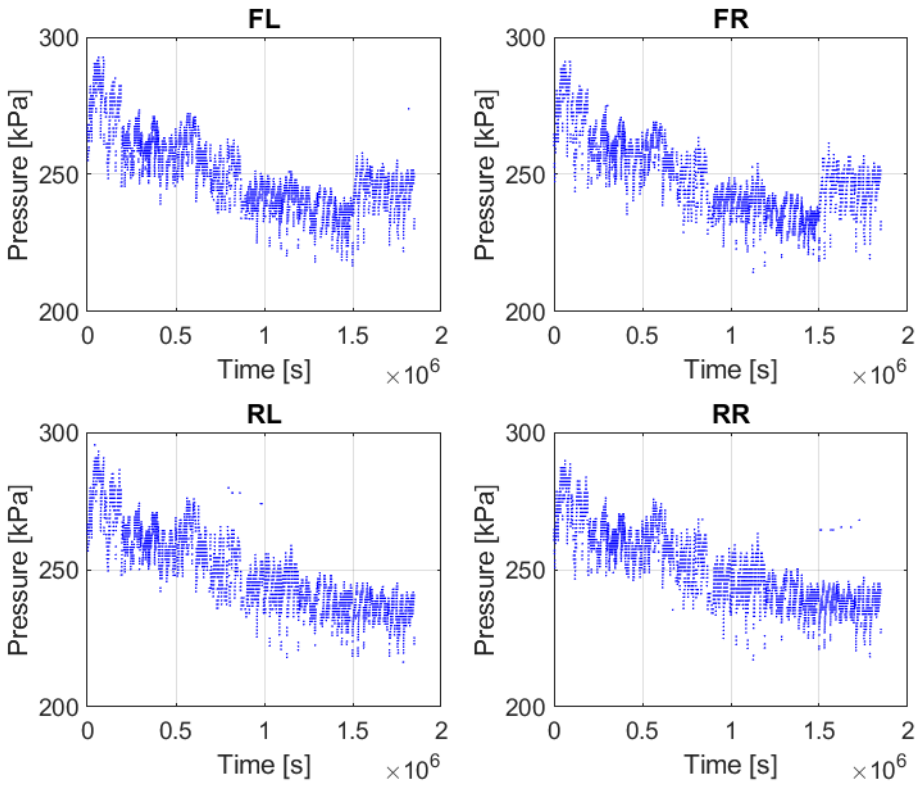

Figure 3.2: This figure shows the pressure signal for all tires for Test Case 2. This signal has been enhanced using the method described in Section 5.1.2.

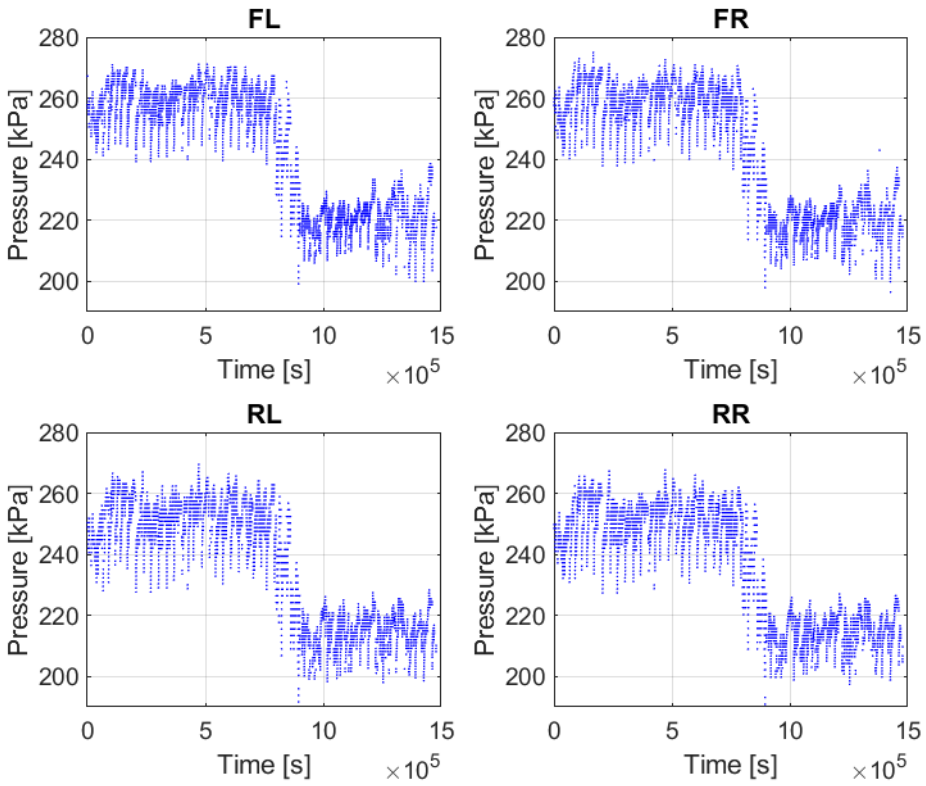

Figure 3.3: This figure shows the pressure signal for all tires for Test Case 3. This signal has been enhanced using the method described in Section 5.1.2.

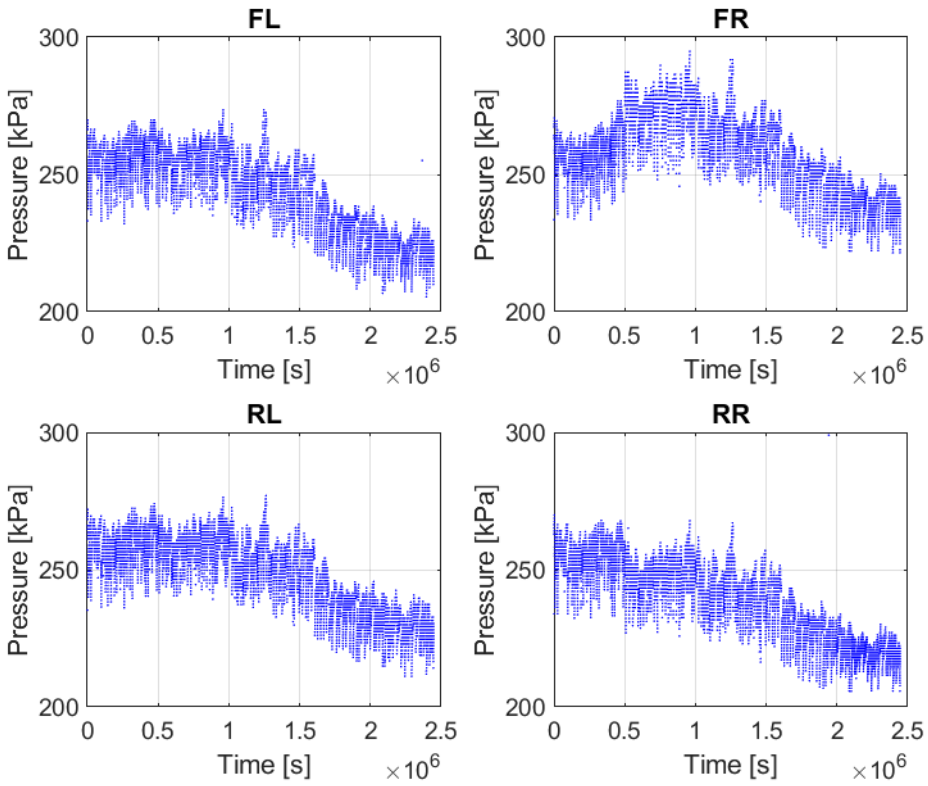

Figure 3.4: This figure shows the pressure signal for all tires for Test Case 4. This signal has been enhanced using the method described in Section 5.1.2.

3.2 Sensors

The models in this thesis uses, as described in Section 1.4, data collected by the sensors available on the cars in the test cases. This means that even though the models in the thesis might benefit significantly from having access to an additional sensor, e.g., an 6-axis IMU, it is not possible to add any sensors, since the models are intended to be used with the currently available sensors. The models in this thesis utilize several in-vehicle sensors, those are: the GPS sensor, the wheel speed sensor, the inertial measuring unit (IMU) and the direct tire pressure monitoring system (dTPMS) sensor.

3.2.1 GPS Sensor

During test drives the vehicles are equipped with external GPS receivers (external in the sense that they are not from OEM). This sensor gives GPS coordinates measurements, but it also gives a GPS-velocity signal that it has calculated from the coordinates. It has a sample frequency of 1 Hz. The vehicle's coordinates are given in the global earth centered coordinate system. This makes it difficult to compare to the the IMU signals, since they are vehicle centered. Therefore the GPS coordinates are converted into North East Down (NED) coordinates using a MATLAB toolbox. This turns the global, polar coordinates, into cartesian coordinates. Since the earth is not flat, there is a slight distortion of the coordinates. However, the test data has been collected in Linköping and the surrounding area, meaning that the NED conversion errors will be negligible.

One issue with the GPS sensor is that there is a slight delay. By comparing it to the wheel speed sensor, it was found that the delay is 1.4 s. To rectify this, the GPS signal is shifted 1.4 seconds forward in the models. It also relies on reception with satellites, meaning that it can sometimes suffer from poor reception giving poor data.

3.2.2 Wheel Speed Sensor

The wheel speed sensor is a tachometer that measures the wheels' angular speed. It has a rather high accuracy and low latency. By multiplying the wheel speed sensor with a fixed radius the wheels' speed can be determined. However, this speed will differ slightly from the ground truth due to: tire slipping and skidding, cornering and change in rolling radius. However, of the three available sensors it will give the closest speed to the ground truth since the GPS speed suffers from low sampling rate and reception issues, and a dead reckoning velocity, calculated with the IMU suffers from long term drift.

3.2.3 Inertial Measuring Unit

The inertial measuring unit (IMU) has three axes. Longitudinal acceleration, lateral acceleration and yaw rate. This means that it lacks the other 3 axes: vertical acceleration, pitch rate and roll rate. The IMU is intended to measure in the vehicle centered coordinate systems. However, due to misalignment during mounting it is usually slightly off, of the true vehicle center. Meaning that it will have a slight bias.

3.2.4 Direct Tire Pressure Monitoring System

The direct Tire Pressure Monitoring System (dTPMS) uses sensors for measuring the tire pressure and tire temperature of each tire. The temperature signal has a resolution of 1°C whereas the pressure signal has a resolution of approximately 5-6 kPa.

3.3 Raw Rolling Radius Signal

The effective rolling radius is calculated using (2.1). However, it requires the velocity of the center of the wheel and estimating it is difficult. To get a simple estimate of the effective rolling radius, one can use the GPS-velocity. The GPS measures the coordinates of the vehicle and calculates an estimate of the velocity of the vehicle. It does not calculate the velocity of individual wheels. This means that it will be accurate when the vehicle is travelling straight, but less accurate when the vehicle is turning. This is because all wheels travels different distances while the vehicle is turning and therefore all tires will have different velocities. The effective rolling radius estimate, calculated using GPS-velocity and wheel speed is in this thesis defined as the raw rolling radius. It is calculated as

$$r_{raw} = \frac{v_{GPS}}{\Omega_{WSS}}, \tag{3.1}$$

where v_{GPS} is the velocity signal from the GPS receiver, Ω_{WSS} is the wheel speed signal from the wheel speed sensor. r_{raw} is "raw" in the sense that it is calculated from the sensor signals without any filtering. Since the raw rolling radius is calculated using signals, it suffers from the measurement noise from the GPS receiver and wheel speed sensor.

3.4 Pre-Compensated Rolling Radius Signal

To limit the scope of the thesis, some compensations have been excluded from the thesis. Instead predefined compensations from NIRA are used. The raw rolling radius signal, in (3.1), deviates from the effective rolling radius when turning as described in Section 3.3. This deviation is compensated for using NIRA's predefined yaw rate compensation to obtain a more accurate estimate of the effective rolling radius. Furthermore, this signal is then also compensated for tire slip using NIRA's predefined compensation to get an estimate of the free-rolling radius. Data points during breaking are simply removed. This is because the amount of breaking torque is unknown, making it difficult to compensate for it. Lastly, this signal is also compensated with respect to the load. After applying these predefined compensations, the signal is filtered using a data quality filter by NIRA which remove poor sample points (obvious outliers etc.). These signals is then also filtered to make sure that only velocities over 40 km/h is included, since lower velocities induce division by zero issues and also the quality of the GPS-signal is worse for lower velocities. The raw rolling radius that has been compensated for yaw rate, tire slip and load and also have been filtered will be called the pre-compensated rolling radius, r_{pc}. This yields a more accurate radius to work with instead of using a completely raw rolling radius where

none of these compensations have been taken into account.

The pre-compensated rolling radius signal can be described by the function in (2.2), where the load and torque have been compensated to a fixed nominal condition. This means that the remaining major, external factors that needs to be compensated for are v, p and T.

$$r_{pc} = f_r(v, p, T, F_{z_0}, M_0, l_{TD}, \theta). \tag{3.2}$$

4 Rolling Radius Estimation

This chapter presents the method, results and discussion of rolling radius estimation.

The effective rolling radius is defined by (2.1) in Chapter 2. The simplest estimate of this radius is to use the raw rolling radius, see Section 3.3. I.e., a radius calculated using GPS-velocity and wheel speed. The wheel speed sensor is quite accurate and has low levels of noise. However, the GPS-velocity has high levels of noise. When dividing two noisy signals with each other the resulting signal gets very noisy, see Figure 4.1. The problem with the high noise intensity is that the change in rolling radius due to tread wear is hard to detect. It is also hard to identify how the rolling radius changes due to external factors (such as vehicle velocity, tire pressure and tire temperature), making the compensations more difficult.

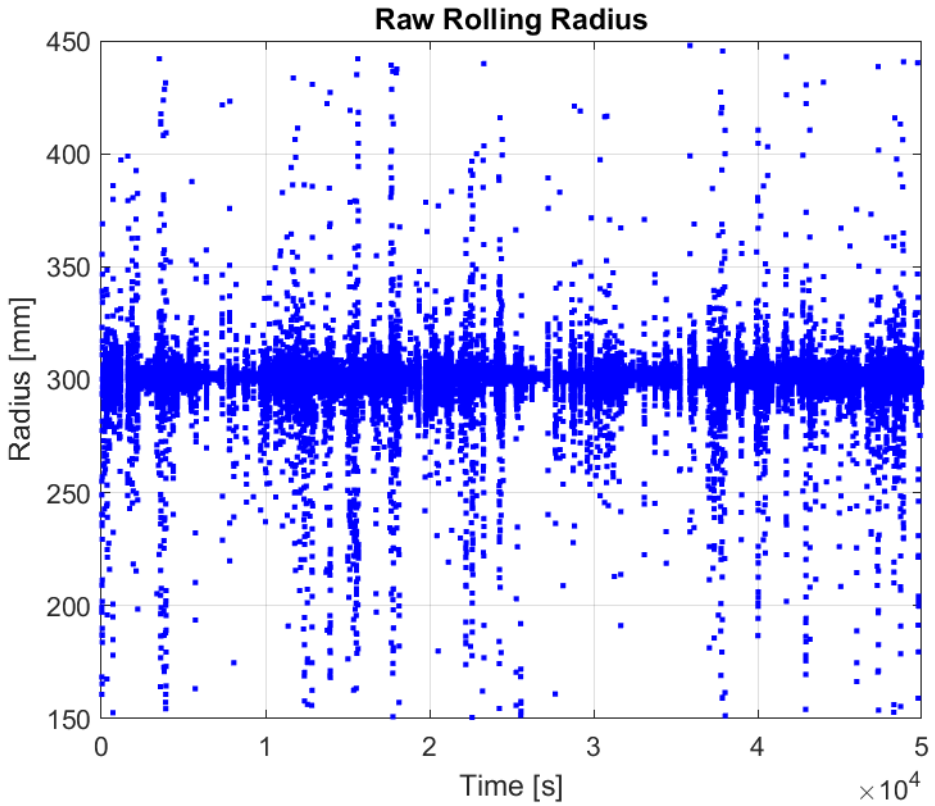

Figure 4.1: This figure shows the raw rolling radius for the FL tire on Test Case 4.

There is therefore a need to achieve a less noisy rolling radius signal. One way of solving this issue is by using sensor fusion. The sensors that are available to use is a GPS and a 3-axis IMU. The three axes of the IMU is the longitudinal acceleration, lateral acceleration and yaw rate. The GPS measures coordinates and calculates an estimate of the velocity. The problem with the raw rolling radius is that the GPS-velocity is too noisy. Therefore the aim of the sensor fusion is to estimate a more accurate

velocity signal so that the resulting rolling radius is less noisy. Estimating velocity using GPS and IMU has been investigated in earlier works, the difference in this case compared with the available literature is that the velocity signal will not be used on its own, but as a mean to achieve a rolling radius. The performance of this velocity estimation is therefore evaluated by analyzing the resulting rolling radius. The goal of this sensor fusion is to achieve a rolling radius that is less noisy than the raw rolling radius. Since the GPS-velocity is calculated using GPS coordinates, it does not add any additional information to the sensor fusion. It is therefore excluded from the sensor fusion.

The GPS coordinates are converted into a NED coordinate system whereas the IMU is in a vehicle centered coordinate system. This results in a need to estimate the vehicle's yaw, and use trigonometric functions to convert the acceleration signals into the global coordinate system. Trigonometric functions are nonlinear, resulting in a need for an Extended Kalman Filter (EKF) [19]. The different coordinate systems are visualized in Figure 4.2.

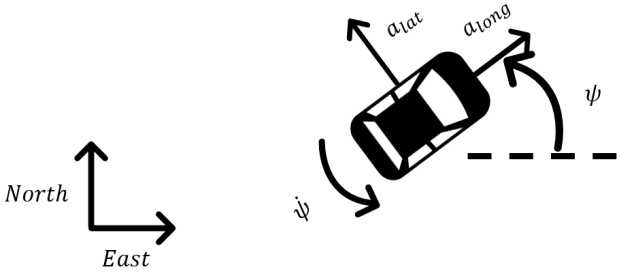

Figure 4.2: This figure visualizes the differences between the NED coordinate system and the vehicle centered coordinate system. It also shows how the IMU signals are described according to the vehicle centered coordinate system.

4.1 Method

The rolling radius is estimated using an Extended Kalman Filter and a corresponding state space. The state space uses a simple particle model. This means that the x position in time step k + 1 is updated by taking the x position in time step k plus the velocity in the x direction during that time step, multiplied by the time step. The y position is updated in a similar fashion. The velocity of the vehicle is defined in the vehicles longitudinal direction, meaning that it needs to be converted using the vehicle's yaw. Since the yaw is unknown it needs to be estimated as well. The velocity is updated by taking the velocity in time step k and adding the acceleration multiplied by the time step. Since an IMU can be misaligned, the longitudinal acceleration is complemented by longitudinal acceleration bias. The yaw state is updated in a similar way using the current yaw plus the yaw rate and the yaw rate bias multiplied by the time step. The acceleration and yaw rate remain unchanged between time steps. These are however updated in the measurement updates instead. The biases also remains unchanged between time steps, and only affected by noise. One issue with using a particle model for a car is that it has no limitation on in which direction the vehicle can move. A car can only travel "forward", and turn by travelling in curves. It cannot move sideways. An alternative would be to use a bicycle model, which gives a more realistic movement of the vehicle. However, a bicycle model requires several additional parameters that needs to be estimated. To reduce complexity of the model this model was therefore avoided. The EKF algortihm is implemented as described in Chapter 2. The states of the EKF model are: eastern position x, northern position y, velocity v, yaw ψ, longitudinal acceleration a, yaw rate $\dot{\psi}$, acceleration bias b_a and yaw rate bias $b_{\dot{\psi}}$. The state vector is defined as

$$X = \begin{bmatrix} x & y & v & \psi & a & \dot{\psi} & b_a & b_{\dot{\psi}} \end{bmatrix}^T. \tag{4.1}$$

The state space model is described by

$$\hat{X}_{k+1|k} = f(X_{k|k}), \tag{4.2}$$

and

$$f(X_{k|k}) = \begin{bmatrix} x_{k+1|k} \\ y_{k+1|k} \\ v_{k+1|k} \\ \psi_{k+1|k} \\ a_{k+1|k} \\ \dot{\psi}_{k+1|k} \\ b_{a\,k+1|k} \\ b_{\dot{\psi}_{k+1|k}} \end{bmatrix} = \begin{bmatrix} x_{k|k} + v_{k|k}\cos(\psi_{k|k})\Delta t \\ y_{k|k} + v_{k|k}\sin(\psi_{k|k})\Delta t \\ v_{k|k} + (a_{k|k} + b_{a\,k|k})\Delta t \\ \psi_{k|k} + (\dot{\psi}_{k|k} + b_{\dot{\psi}_{k|k}})\Delta t \\ a_{k|k} \\ \dot{\psi}_{k|k} \\ b_{a\,k|k} \\ b_{\dot{\psi}_{k|k}} \end{bmatrix}. \tag{4.3}$$

This results in the state transition Jacobian function

$$\frac{\partial f}{\partial X} = \begin{bmatrix} 1 & 0 & \cos(\psi)\Delta t & -v\sin(\psi)\Delta t & 0 & 0 & 0 & 0 \\ 0 & 1 & \sin(\psi)\Delta t & v\cos(\psi)\Delta t & 0 & 0 & 0 & 0 \\ 0 & 0 & 1 & 0 & \Delta t & 0 & \Delta t & 0 \\ 0 & 0 & 0 & 1 & 0 & \Delta t & 0 & \Delta t \\ 0 & 0 & 0 & 0 & 1 & 0 & 0 & 0 \\ 0 & 0 & 0 & 0 & 0 & 1 & 0 & 0 \\ 0 & 0 & 0 & 0 & 0 & 0 & 1 & 0 \\ 0 & 0 & 0 & 0 & 0 & 0 & 0 & 1 \end{bmatrix}. \tag{4.4}$$

The measured signals are the east and north coordinates (converted into cartesian coordinates) and the longitudinal acceleration and yaw rate, giving a signal Y as

$$Y = \begin{bmatrix} x & y & a & \dot{\psi} \end{bmatrix}^T. \tag{4.5}$$

Since all measured signals are states, the measurement function is linear and can be written as

$$h(X) = \begin{bmatrix} 1 & 0 & 0 & 0 & 0 & 0 & 0 & 0 \\ 0 & 1 & 0 & 0 & 0 & 0 & 0 & 0 \\ 0 & 0 & 0 & 0 & 1 & 0 & 0 & 0 \\ 0 & 0 & 0 & 0 & 0 & 1 & 0 & 0 \end{bmatrix} \begin{bmatrix} x \\ y \\ v \\ \psi \\ a \\ \dot{\psi} \\ b_a \\ b_{\dot{\psi}} \end{bmatrix} = HX. \tag{4.6}$$

Since the measurement function is linear, the jacobian will be the constant matrix H:

$$h'(X) = H. \tag{4.7}$$

The system uses both measurements from the GPS and IMU. These sensors do however have different sampling rates. The GPS has a sampling rate of 1 Hz and the IMU has a sampling rate of 10 Hz. This means that there will be two different kinds of measurements updates. There will be a full measurement update when the GPS receives an update, and in between those there will be partial updates using only IMU measurements. This EKF will use the algorithm described in Section 2.2.1, with the only difference being that there will be a different h functions depending on if there has been

a GPS update in that time step. The full measurement function is

$$h_{GPS}(X) = \begin{bmatrix} 1 & 0 & 0 & 0 & 0 & 0 & 0 & 0 \\ 0 & 1 & 0 & 0 & 0 & 0 & 0 & 0 \\ 0 & 0 & 0 & 0 & 1 & 0 & 0 & 0 \\ 0 & 0 & 0 & 0 & 0 & 1 & 0 & 0 \end{bmatrix} \begin{bmatrix} x \\ y \\ v \\ \psi \\ a \\ \dot{\psi} \\ b_a \\ b_{\dot{\psi}} \end{bmatrix}, \tag{4.8}$$

and the partial, IMU only measurement function is

$$h_{IMU}(X) = \begin{bmatrix} 0 & 0 & 0 & 0 & 1 & 0 & 0 & 0 \\ 0 & 0 & 0 & 0 & 0 & 1 & 0 & 0 \end{bmatrix} \begin{bmatrix} x \\ y \\ v \\ \psi \\ a \\ \dot{\psi} \\ b_a \\ b_{\dot{\psi}} \end{bmatrix}. \tag{4.9}$$

4.2 Result

The EKF has three tunable parameters. Those are the three covariance matrices Q, R and P. Tuning and testing resulted in a process covariance matrix of

$$Q = \text{diag}(\begin{bmatrix} 0 & 0 & 10^{-2} & 10^{-4} & 10^{-3} & 10^{-3} & 10^{-9} & 10^{-12} \end{bmatrix}), \tag{4.10}$$

and a measurement covariance matrix of

$$R = \text{diag}(\begin{bmatrix} 10^{-1} & 10^{-1} & 10^{-3} & 10^{-10} & 10^{-10} \end{bmatrix}). \tag{4.11}$$

Finally the covariance matrix was found to be

$$P = \text{diag}(\begin{bmatrix} 10 & 10 & 5 & 10\frac{\pi}{180} & 2 & 5\frac{\pi}{180} & 0.1 & 0.1 \end{bmatrix}). \tag{4.12}$$

The EKF was tried and tested on Test Case 4, on the first 15,000 seconds. The reason for not testing it on the entire test case was to reduce computational time and development time. This resulted in an estimated velocity, see Figure 4.3. Since there is no ground truth, the EKF velocity needs to be compared with either the wheel speed sensor or the GPS-velocity. The wheel speed sensor has a high sampling frequency and low noise, it does however assume a fixed rolling radius to convert angular speed to vehicle velocity. This means that it is accurate when it comes to variation in velocity but less accurate for absolute values of the velocity. The GPS signal is in contrast more reliable for absolute values, but can miss quick variations. The figure shows how the EKF overall follows the wheel speed and GPS signals rather well.

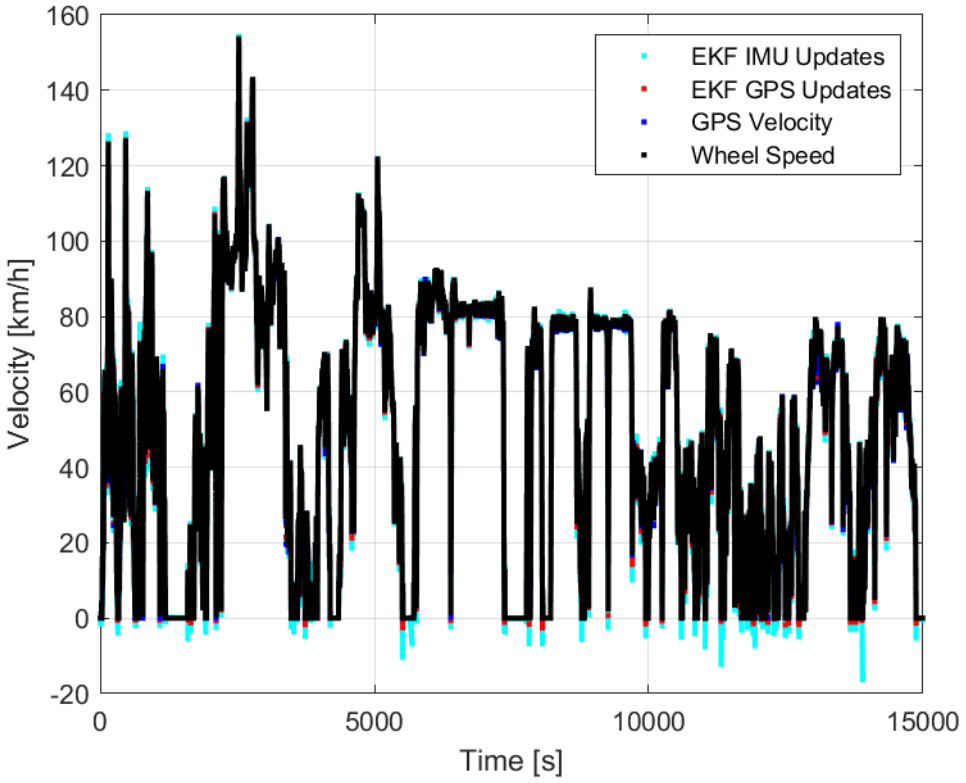

Figure 4.3: This figure shows the velocity estimated by the EKF. The black dots are the wheel speed sensors multiplied by a fixed radius, the blue dots are the GPS-velocity and the red and cyan dots are the EKF estimated velocities. The red dots are the time steps where the EKF has received a GPS measurement update and the cyan dots is when it is only utilizing IMU measurements.

Figure 4.3 shows how the EKF sometimes results in negative velocities, while the wheel speed and GPS does not. Negative velocity means that the vehicle is travelling in reverse. The wheel speed sensor never results in negative velocities since it is a tachometer, which cannot measure angular direction, .i.e., it cannot tell when the vehicle is moving in reverse. The GPS-velocity signal is technically an estimate of the vehicle's speed, calculated by the GPS receiver. The vehicle's speed is a non-negative scalar, which means that it will always give positive values even when the vehicle is travelling in reverse. There is a signal that indicate if the vehicle is going in reverse. Meaning that both GPS and wheel speed can be corrected to account for negative velocities. However, low speed will in general cause issues due to division of small numbers, and the low velocity points will be filtered out; meaning that this discrepancy does not matter. Figure 4.4 shows a smaller segment of Figure 4.3. It shows that the EKF follows the other sensors well but with slight overshoots.

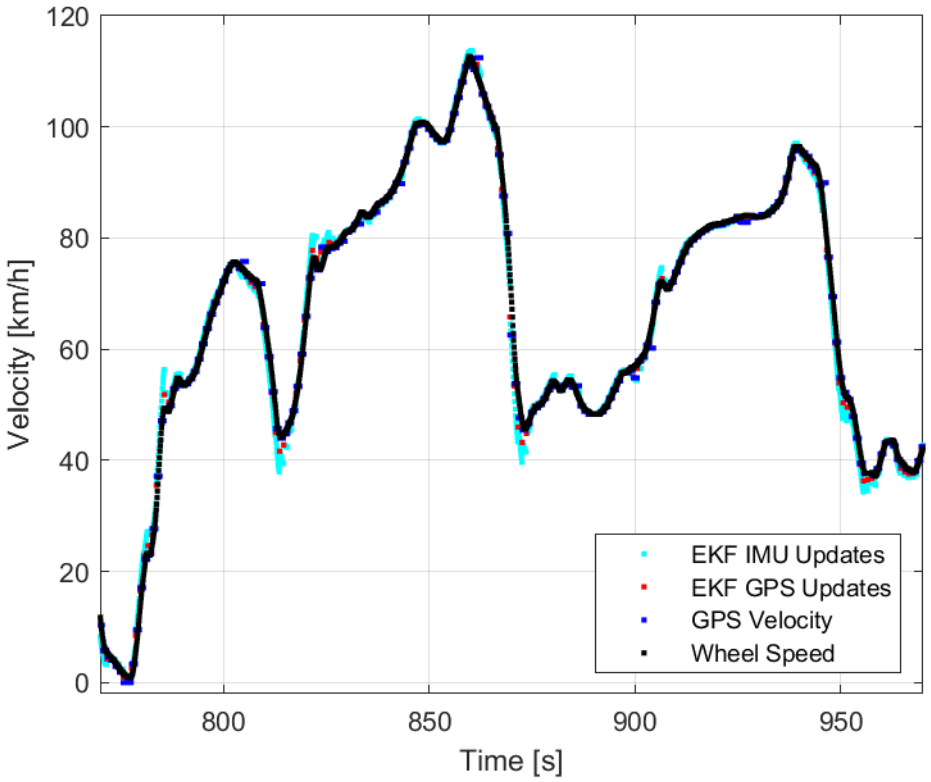

Figure 4.4: This figure shows the velocity estimated by the EKF.

Using the estimated velocity from the EKF, the rolling radius can be calculated. This rolling radius and the raw rolling radius is shown in Figure 4.5. From this figure it is clear that the EKF radius has less and smaller outliers than the raw rolling radius. Which would indicate that the EKF radius is better than the raw rolling radius. However, if one applies NIRA's data quality filtering and velocity filter (v > 40 km/h), the results are different, see Figure 4.6. The raw radius has still more outliers but it is clear that the overall noise level is higher for the EKF. Table 4.1 shows the values for the standard deviation from the raw rolling radius signal and the rolling radius signal estimated using the EKF. The table contains the values from both before and after the filtering procedure, described above. From this table it can be determined that the raw rolling radius yields a better and more stable rolling radius signal after filtering has been applied.

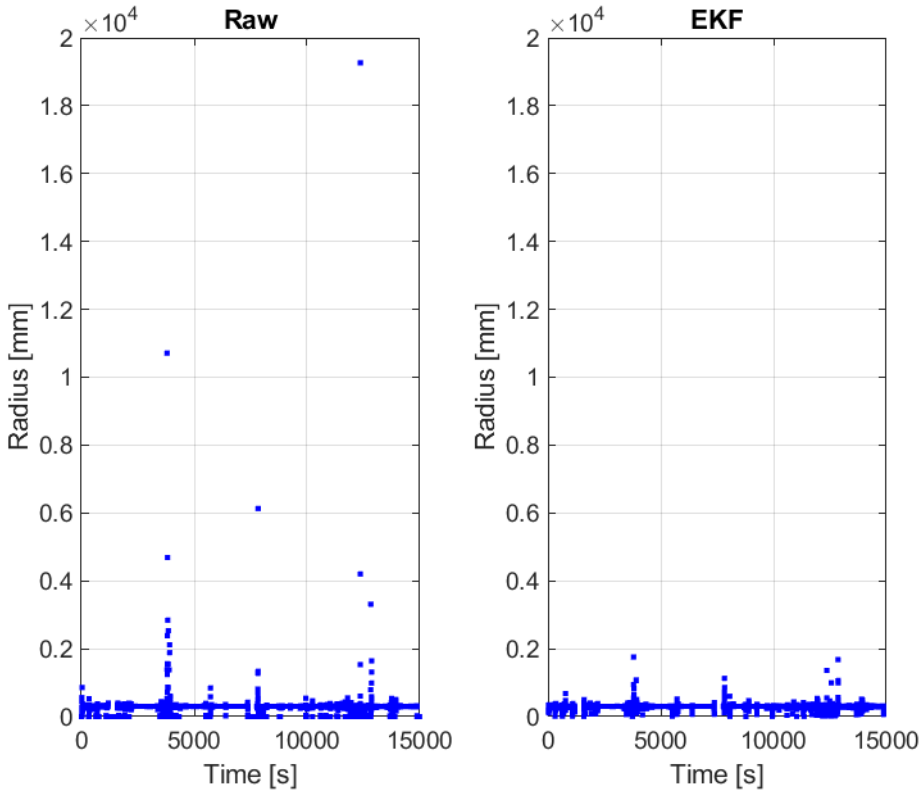

Figure 4.5: This figure compares the raw rolling radius and the rolling radius calculated using EKF. The raw rolling radius signal has no filtering. The EKF signal has been filtered to only include points with GPS measurement updates.

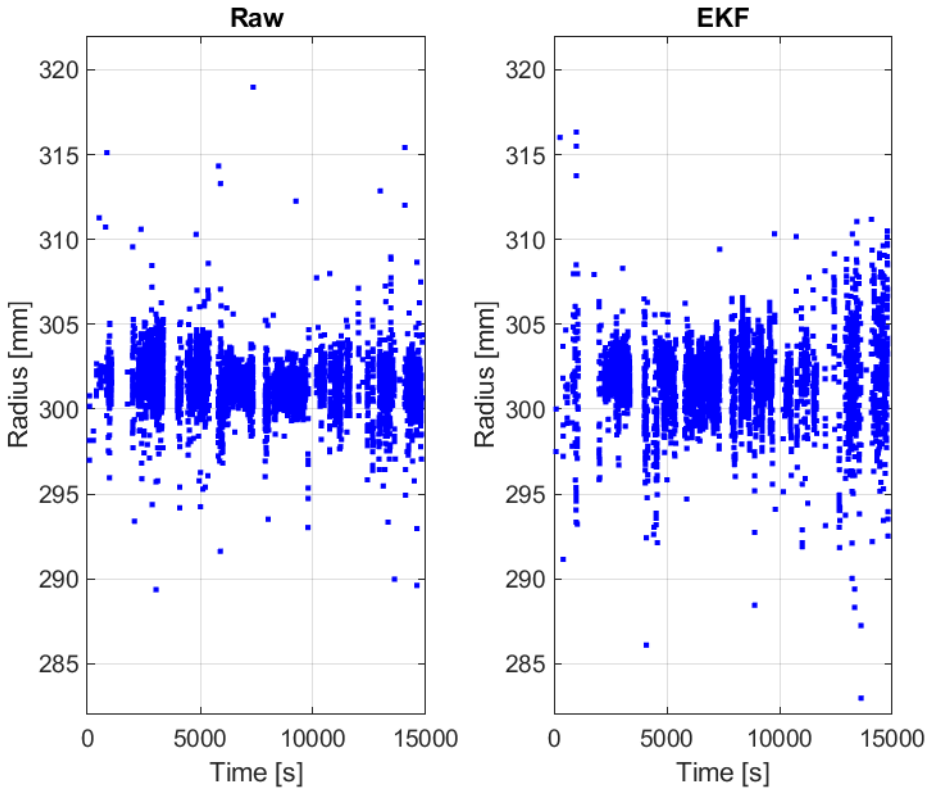

Figure 4.6: This figure compares the raw rolling radius and the rolling radius calculated using EKF. The signals have both been filtered using the NIRA data quality filter. All points with a velocity under 40 km/h have also been removed.

Table 4.1: The standard deviation for the raw rolling radius signal and the rolling radius signal estimated from the EKF.

	Raw Rolling Radius [mm]	EKF Rolling Radius [mm]
Without filtering	452.3592	43.7462
With Filtering	1.3112	2.0312

The least noisy regions in Figure 4.6 are around 7,000 seconds, this is because the velocity during this period is almost constant, see Figure 4.3. This period is shown in Figure 4.7. During this period it seems that the EKF radius oscillates with the oscillations in velocity. This is somewhat of an expected behavior, since the radius increases with speed. However, the amplitude in this case is larger than it is expected to be. The figure also shows how the increase and decrease in velocity follows the acceleration signal.

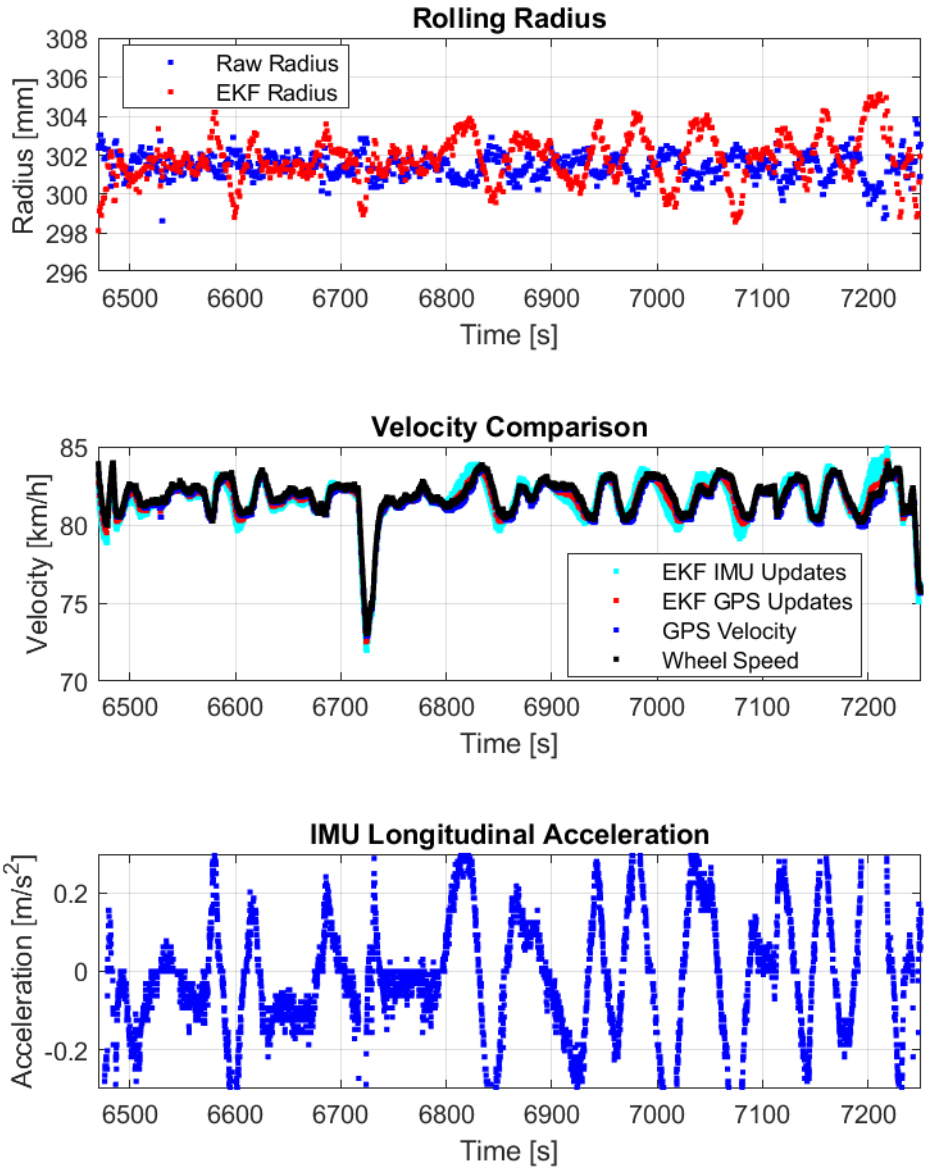

Figure 4.7: This figure compares the raw rolling radius and the rolling radius calculated using EKF.

4.3 Discussion

Upon further investigation of Figure 4.7 a troublesome behavior was discovered. Figure 4.8 shows an even smaller time interval where this behavior is clearer. The figure shows how both the wheel speed sensor and the GPS velocity is giving constant signals while the EKF shows a constant decrease in velocity. Since both the GPS and wheel speed sensor gives a constant velocity, the ground truth is probably also constant in this interval. One can see in the figure how the red dots, those that have a GPS measurement update tries to follow the ground truth, but the cyan dots, that only rely on the IMU wants to decelerate. The reason for this behavior is simply that the IMU is sending a signal of negative acceleration, see subplot three in Figure 4.8. This is a major issue since the ground truth clearly does not decelerate in this interval. The measured mean longitudinal acceleration in this interval is -0.1 m/s^2. Over this 50 second interval, an average deceleration of -0.1 m/s^2 would result in a velocity decrease of 50 km/h, comparing this to the fact that the GPS and wheel speed velocities only decreases by 2 km/h in the same time interval, it is clear that the IMU is giving a too large signal. One reason for this behaviour could be that the vehicle is traveling at an incline. This means that the IMU would be measuring a component of the gravitational acceleration, resulting in a faulty longitudinal acceleration signal. This is most likely the reason for the poor radius estimation performance in Figure 4.6. This means that without knowing the slope of the ground, and the vehicle's pitch, the IMU cannot be compensated for this issue. It is clear that in cases like this; the IMU reduces the performance of the EKF, and simply using the GPS velocity would result in better performance.

Methods for accurate vehicle attitude estimation have been discussed in [21], however this solution assumes a 6-axis IMU. The test data available to this thesis only has a 3-axis IMU, this fact rules out those kinds of solutions. It seems that given the available sensors, this approach of estimating the rolling radius using sensor fusion of GPS and IMU signal is not a beneficial method.

The goal of the sensor fusion was to estimate a rolling radius that is less noisy than the raw rolling radius. Since, the result does not fulfil this goal, this rolling radius estimated using EKF will not be used in the compensation model. Instead the raw rolling signal will be used.

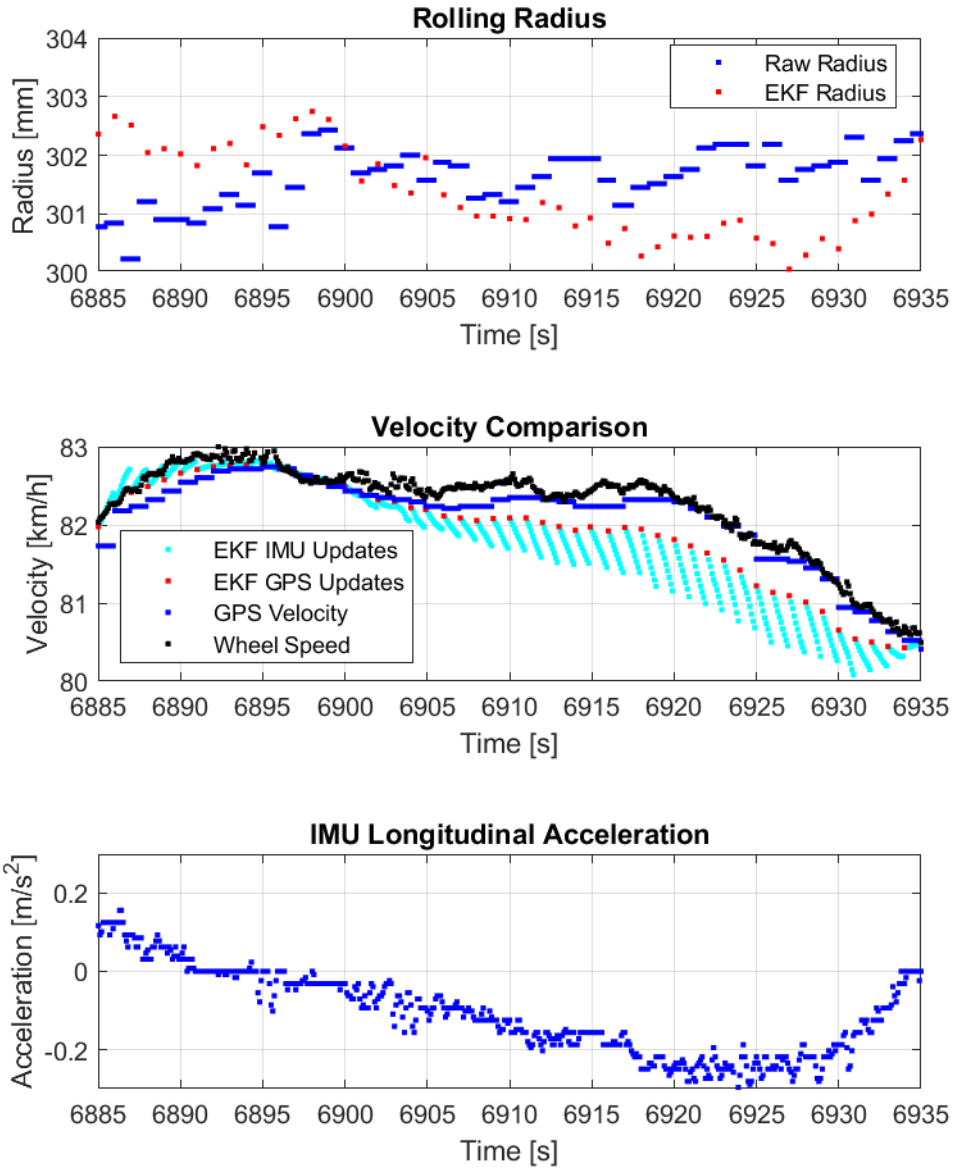

Figure 4.8: This figure compares the raw rolling radius and the rolling radius calculated using EKF.

5 Rolling Radius Compensation

In this chapter methods for compensating a rolling radius signal with respect to velocity, tire pressure and tire temperature are investigated. These compensations were performed on the pre-compensated rolling radius signal. I.e., the signal that have been calculated using GPS-velocity and wheel speed, and then been pre-compensated for yaw rate, slip and load and also filtered, see Section 3.4. The compensation results are presented and discussed. This chapter covers compensation of a single tire set at a time. Meaning that the compensation factors are trained and validated on the same test case. Some processing of certain signals are made and these modifications are also described below.

5.1 Method

This section presents the method used to compensate the pre-compensated rolling radius signal. The compensation consists of several steps, those are: noise reduction, pressure signal enhancement, handling of tire growth, regression model, linear and quadratic compensation models, performance evaluation and finally, validation.

5.1.1 Noise Reduction

The raw rolling radius signal calculated as described in Section 3.3 is affected by several factors that make it deviate from the nominal rolling radius. This deviation is reduced by applying NIRA's pre-compensation, that compensates for yaw rate, load and slip. Another factor that causes it to deviate from the nominal rolling radius is measurement noise. The wheel speed sensor has rather low levels of noise but the GPS has high levels of noise. To be able to evaluate compensated rolling radius decrease due to tread wear, the noise needs to be significantly reduced.

Measurement noise is in general so called white noise. White noise has Gaussian distribution meaning that the deviations from the true mean is normally distributed. A good estimate of the true mean is to take the average value of the data set. Since the change in rolling radius over time due to tread wear is desired, the averages needs to be applied in shorter segments as to not lose the time dependency. These segments were set to 10,000 s. An issue with taking the averages of these segments is that the effects of outliers in the data set will be significant. These effects are shown in Figure 5.1 where both the averages and the medians are calculated in segments. The subplot *Without Filtering* (meaning that neither the data quality filtering nor the velocity filtering, explained in Section 3.4, have been applied to the rolling radius signal) shows how the average approach is sensitive to outliers. Although, after applying the filtering there is a minor difference between taking the average or calculating the medians, which can be seen in Figure 5.1 in the subplot *With Filtering*. Figure 5.2 shows a zoomed in version of the subplot *With Filtering* which shows how the pre-compensated rolling radius decreases slightly over time, due to several factors one of which is tread wear. This zoomed in figure also amplifies the result of that there is a minor change between the average and median approach after applying the filtering. This means that after filtering medians and averages get similar results. However, medians are still the preferred method since it can handle outliers better. And one cannot guarantee that the filtering is always as effective at removing outliers as in this case. Medians will effectively reduce the Gaussian noise and leave a good estimate of the mean of the signal over that time segment. Any underlying biases in the data will however remain after taking the medians. These biases come from the change in tire conditions compared to nominal conditions, e.g., a change in tire pressure. They need to be removed to be able to use the compensated rolling radius signal to estimate tread wear.

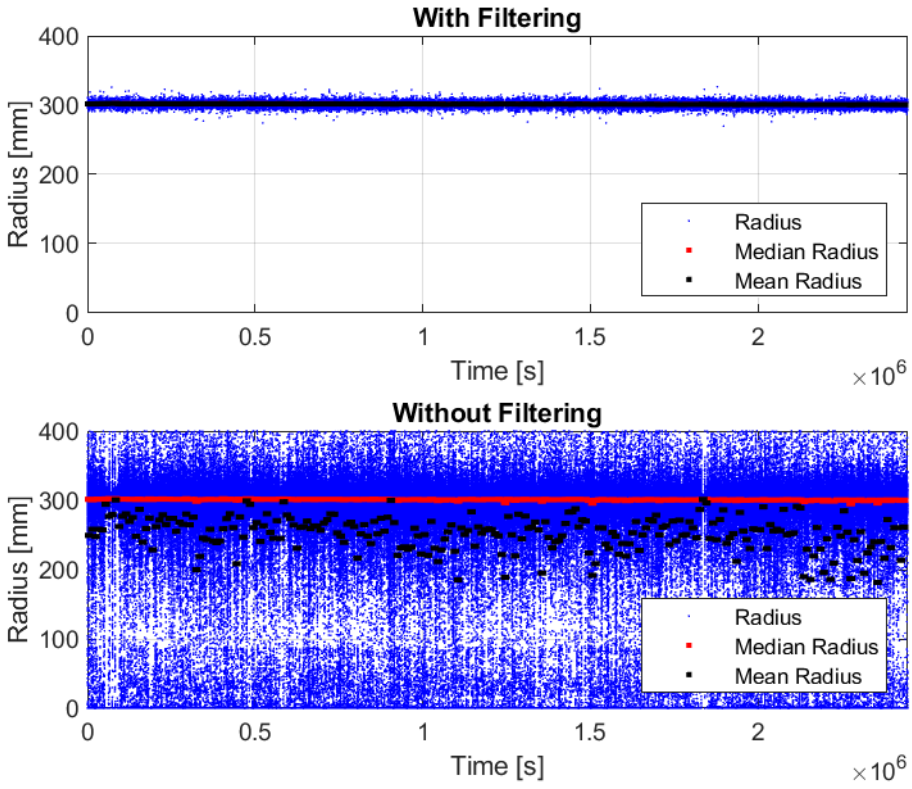

Figure 5.1: Figure illustrating the impact of the data quality filtering and the velocity filtering and how this affects the usage of an average approach in segments compared to a median approach in segments. For the FL tire on Test Case 4.

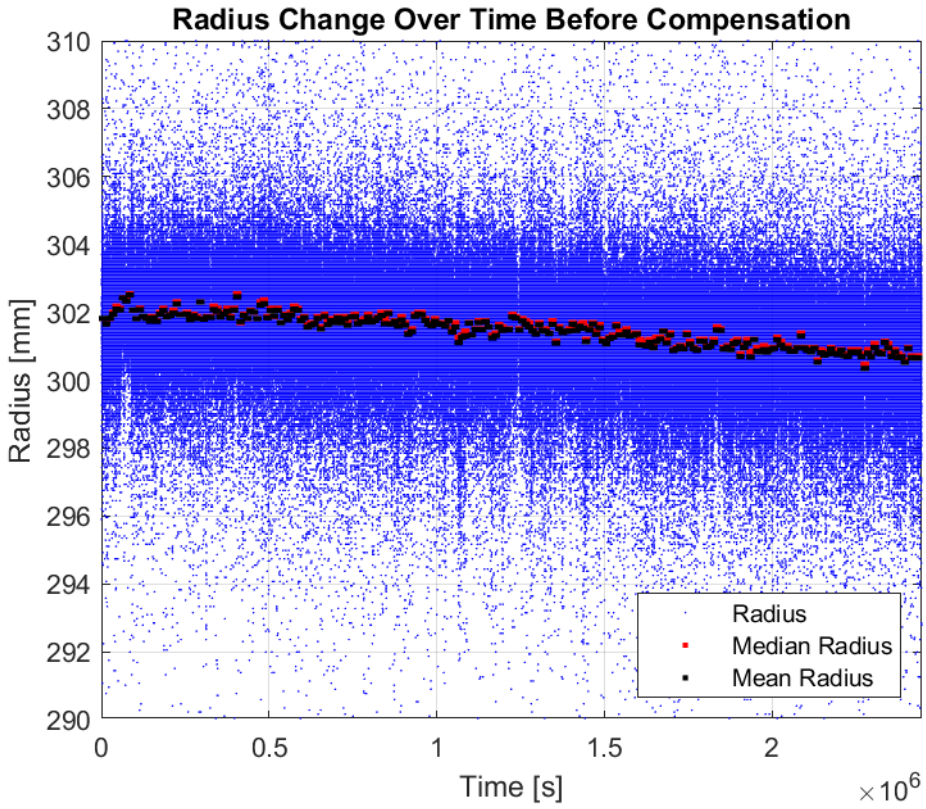

Figure 5.2: Zoom of subplot *With Filtering* in Figure 5.1 giving a clearer picture of the minor difference between using averages och medians if the filtering is applied.

5.1.2 Pressure Signal Enhancement

One issue with trying to compensate for changes in tire pressure is the low resolution of the tire pressure signal from the dTPMS sensor in the available data set. As mentioned in Section 3.2.4 the resolution of the pressure signal is around 5-6 kPa. This problem is illustrated by Figure 5.3 where the low resolution of the pressure signal can be seen. However, the temperature signal has a significantly higher resolution 1 °C, as can be seen in the figure.

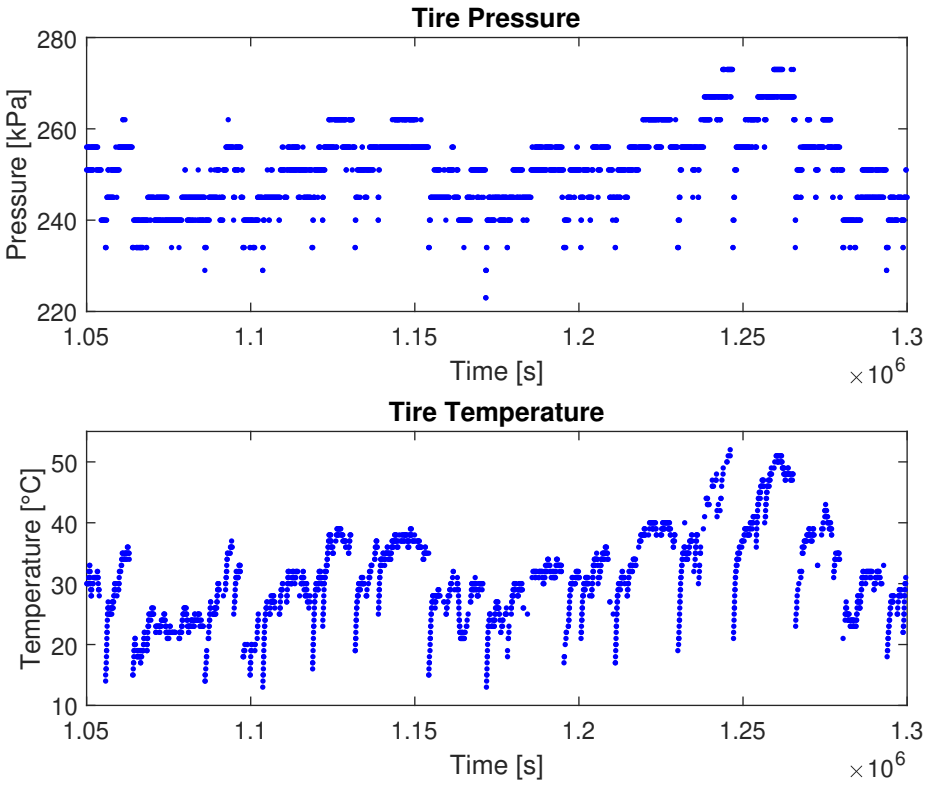

Figure 5.3: Resolution of the raw tire pressure signal and tire temperature. For the FL tire on Test Case 4.

The figure clearly shows that there is a relationship between the tire temperature and the tire pressure. This relationship can be explained by the ideal gas law. The tire pressure signal is therefore improved by using the tire temperature signal to model a tire pressure signal with higher resolution. This is done using least squares regression on an affine model in batches of 100,000 s (5% of data set). The model is on the form

$$\hat{p} = a \cdot T + b, \tag{5.1}$$

where $\hat{p}$ is the modelled pressure, T is the temperature and, a and b are coefficients that are determined using linear least squares regression. The resulting pressure signal when applying this least squares regression can be seen in Figure 5.4. An issue with this method is that the new pressure signal becomes linear dependent on the temperature signal. Linear dependency means that both the pressure signal and temperature signal cannot be included in a linear least squares regression model, since the A matrix, in (2.21), would become singular and noninvertible. However, since (5.1) is recalculated every 100,000 s the signals are not linearly dependent over the entire data set. The relationship between tire pressure and tire temperature is not constant over time for several reasons. One is if the tire is manually deflated or inflated. By recalculating the model in (5.1) these changes in pressure-temperature relationship are accounted for and the signals are not linearly dependent.

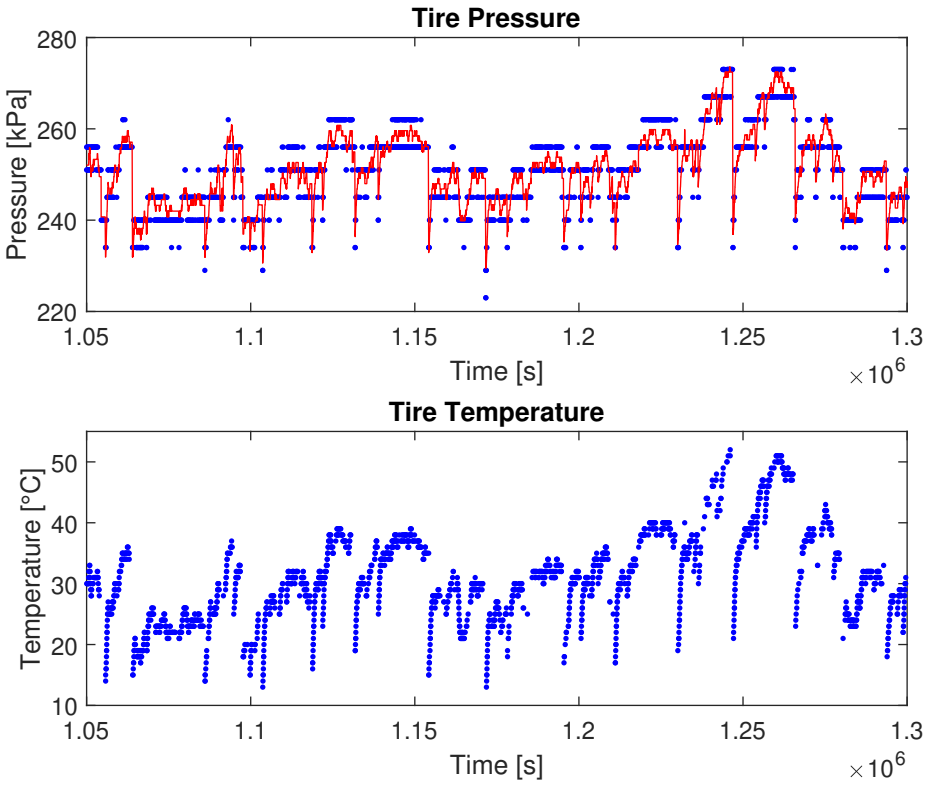

Figure 5.4: Resolution of the modeled tire pressure signal and tire temperature.

5.1.3 Initial Tire Growth

Initial tire growth is a tire phenomenon that occurs at an initial stage of a tire's life cycle. When a tire is new it slightly expands for the first part of its lifetime. This phenomenon is illustrated in Figure 5.5, where the tire growth is present for approximately the first 500,000 s of the total driving time on the tires. This gives a nonlinear behavior at the initial stage. This nonlinearity will significantly affect the performance of linear regression. Therefore this initial part of the data sets is excluded when calculating dependency factors. To get an estimate of the tire wear of the entire data set; a linear line is fitted to the data after the growth phenomenon and then extrapolated to cover the first 500,000 s. This way, one can estimate the rolling radius decrease as if there was no initial tire growth.

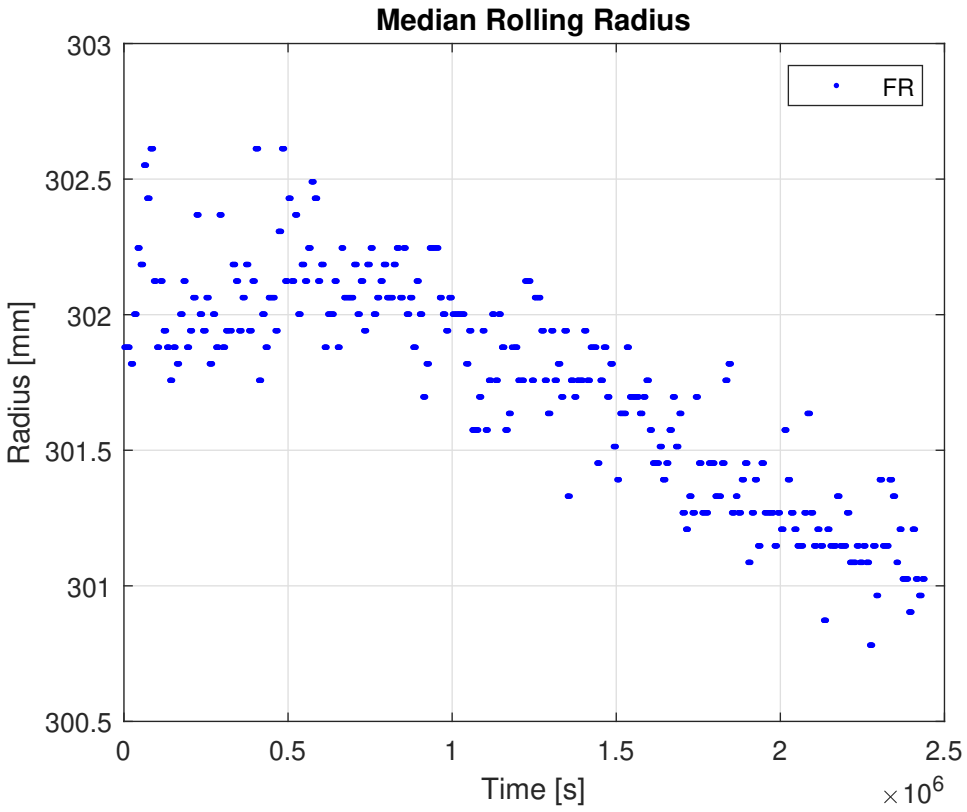

Figure 5.5: This figure shows the medians of the pre-compensated rolling radius for the FR tire of Test Case 4. It clearly shows the initial tire growth phenomenon during the first 500,000 s.

5.1.4 Radius Dependency on External Factors

The effective rolling radius of a tire is dependent on several factors. One of them is the vehicle's velocity, this dependency can be explained by the centrifugal force of the tire making it expand. However, an alternate argument is that at higher speeds the tire endures greater forces and torques meaning that the effective rolling radius would decrease. The velocity of the vehicle could also affect the effective rolling radius through liftforce and downforce. If a vehicle's lift force is greater than its downforce; the vehicle would lift with speed meaning that the effective rolling radius should increase. If instead the downforce is greater than the liftforce, the effective rolling radius would decrease with increasing speed.

The effect of tire pressure on the effective rolling radius is rather clear, increasing the pressure will increase the volume which also increases the effective rolling radius. The effect of tire temperature is often correlated with tire pressure; since both the tire temperature and tire pressure increases over time while driving. However, the tire pressure can be changed by manually inflating the tires, which does not affect the tire temperature. The tire temperature is also affected by the ambient temperature. During the winter the ambient temperature is lower which increases the amount of cooling of the tires; making them overall colder than if they are used in the summer. Tire temperature could also affect the tires' material properties; making it less or more stiff, which could affect the tires' effective rolling radius as well. This thesis will not investigate the causes for the effective rolling radius dependencies, but only the effects of them.

Therefore, before investigating different compensation models, the relation between the different external factors and the effective rolling radius are scrutinized to detect if a compensation with regard to the specific external factors would yield a difference in effective rolling radius. This investigation was performed using the pre-compensated rolling radius signal, by simply plotting the it against each external factor.

One way of compensating the signal is to use a linear model. I.e., to model the pre-compensated rolling radius as an affine function of one or more variables with corresponding coefficients and then compensating by using those coefficients as compensations factors. An alternate way is to use quadratic models. This could fit velocity models especially well; since kinetic energy increases with the velocity squared. To evaluate if the relationship between pre-compensated rolling radius and each external factor is linear or quadratic, they have been plotted against each other and both a linear and a quadratic fit has been applied to the data using the MATLAB-function *fit* from the MATLAB toolbox Curve Fitting Toolbox. The *fit* function uses linear least squares to fit a line to the data. Using a linear or quadratic compensation model is only reasonable if there is a linear or quadratic relationship between the pre-compensated rolling radius and a given external factor. In reality there is most certainly no such relationships between pre-compensated rolling radius and external factors, but the behavior might be quite linear or quadratic in the operating region making the compensation method feasible. A drawback of using least squares to fit a line to the data is the effects of outliers. Therefore, an approach using median was also used to get an alternative visualization of the dependency.

5.1.5 Compensation Method

The compensation of the pre-compensated rolling radius consists of two steps. First is the regression model and the determination of the parameters (k_v, k_p, k_T and k_{TD}). The second step is to use the parameters determined in the regression to compensate the rolling radius.

A regression model is a model that tries to fit a polynomial function, $aK = b$, to an arbitrary data set of inputs, a, to an output, b. The aim of the regression model is to estimate the coefficients, K, that minimizes the squared errors between the modelled output and the actual output. This is done using linear least squares, as described in Section 2.3. In this case the output, b, is the pre-compensated rolling radius signal, r_{pc}, and the inputs, a, are the sensor signals (T, p, v) and measured tread depth (l_{TD}). This thesis has developed several functions that describes how the inputs (T, p, v, l_{TD}) relates to the output, r_{pc}. An example of a regression model is

$$\hat{r}_{vp} = k_v \cdot v + k_p \cdot p + m. \tag{5.2}$$

where k_v is the velocity dependency factor and k_p is the tire pressure dependency factor, on the pre-compensated rolling radius. The vehicle's GPS-velocity is denoted as v, p is the tire pressure, and m is a constant bias. $\hat{r}_{vp}$ is the linear model that is fitted to the data. This model describes how the tire pressure and vehicle velocity relates to the pre-compensated rolling radius. This means that the factors k_v and k_p describe the pre-compensated rolling radius dependency on vehicle velocity and tire pressure respectively.

The actual compensation of the pre-compensated rolling radius is done by subtracting the dependency factors multiplied by the corresponding variable from the pre-compensated rolling radius. E.g.,

$$r_{comp,vp} = r_{pc} - k_v \cdot v - k_p \cdot p, \tag{5.3}$$

where $r_{comp,vp}$ is a rolling radius that has been compensated for velocity and pressure.

The medians applied in Figure 5.2 is only used for evaluation. Any compensation model needs to be applied to the data without medians; this is because the noise in the pre-compensated rolling radius comes from shorter events, such as tire pressure increasing during driving. These events are lost after taking the medians. Therefore the compensation models are developed using the unprocessed signal (i.e., without medians), then applied to the pre-compensated signal and then new medians are calculated over 10,000 s segments. These are then compared to the pre-compensated signal to evaluate if the compensation removed noise and unwanted rolling radius effects.

5.1.5.1 Linear Model

The final linear model is called *Linear* and consists of the regression model

$$\hat{r}_l = k_v \cdot v + k_p \cdot p + k_T \cdot T + k_{TD} \cdot l_{TD} + m, \tag{5.4}$$

where k_T is the temperature dependency factor and k_{TD} is the tread depth dependency factor. l_{TD} is the tread depth. $\hat{r}_{lin}$ is the linear model that is fitted to the data. l_{TD} was produced by interpolating actual measurements of tread depth. This regression model was developed by iteratively adding an additional variable to the model, and assessing the performance in relation to the other models. Subtracting the dependency factors obtained from (5.4) times the corresponding variable from the pre-compensated rolling radius gives the compensation model is on the form

$$r_{comp,l} = r_{pc} - k_v \cdot v - k_p \cdot p - k_T \cdot T. \tag{5.5}$$

$r_{comp,l}$ is the linear compensated rolling radius and r_{pc} is the pre-compensated rolling radius. Unlike the k_v, k_p and k_T factors, the k_{TD} is not included in the compensation model. This is because if it was included, the reduction in pre-compensated rolling radius due to tread wear would be removed from the compensated rolling radius. It is only included in the least squares regression model to get more accurate k_v, k_p and k_T factors.

5.1.6 Quadratic Compensation Model

An alternative regression model to the linear regression model in (5.4) is to use a quadratic regression model. This quadratic regression model can be quadratic with regard to different external factors. The *Linear* model in (5.4) will be compared with two quadratic regression models, the *V-Quadratic* model and the *Quadratic* model. In general any arbitrary data set will get a better fit when using a quadratic regression model compared with a linear regression model. This is because a second order model has more degrees of freedom compared to a linear one; meaning that it has a better ability to adapt to the data. This is however only true if one validates the model on the training data. This could mean that even though a quadratic model might fit better on the training data, a linear model might perform better in reality when one does not validate the model on the training data. This could be because a quadratic model has a higher tendency to overfit. There is therefore a need to compare and validate a quadratic and linear model, that does not validate on the training data; this is done by using cross validation.

5.1.6.1 V-Quadratic Model

The *V-Quadratic* model is only quadratic in regards to velocity. The reason for this is because kinetic energy depends on the velocity squared, meaning that this model does in a sense depend linearly on the kinetic energy. This *V-Quadratic* regression model is defined as

$$\hat{r}_{vq} = q_v \cdot v^2 + k_v \cdot v + k_p \cdot p + k_T \cdot T + k_{TD} \cdot l_{TD} + m, \tag{5.6}$$

where q_v is the quadratic velocity dependency factor. Subtracting the dependency factors obtained from (5.6) times the corresponding variable from the pre-compensated rolling radius gives the *V-Quadratic* compensation model is on the form

$$r_{comp,vq} = r_{pc} - q_v \cdot v^2 - k_v \cdot v - k_p \cdot p - k_T \cdot T. \tag{5.7}$$

5.1.6.2 Quadratic Model

The *Quadratic* regression model is quadratic in regards to all external factors except the tread wear, this is because the effects of tread wear on the pre-compensated rolling radius is assumed to be linear. Neither of the quadratic models does include the quadratic cross terms, i.e., $v \cdot p$. The *Quadratic* regression model is defined as

$$\hat{r}_q = q_v \cdot v^2 + k_v \cdot v + q_p \cdot p^2 + k_p \cdot p + q_T \cdot T^2 + k_T \cdot T + k_{TD} \cdot l_{TD} + m, \tag{5.8}$$

where q_p is the quadratic tire pressure dependency factor and q_T is the quadratic tire temperature dependency factor. The *Quadratic* compensation model is obtained in the same way as the *V-Quadratic* compensation model, by subtracting the acquired dependency factors times the corresponding variable from the pre-compensated rolling radius. This gives the *Quadratic* compensation model on the form

$$r_{comp,q} = r_{pc} - q_v \cdot v^2 - k_v \cdot v - q_p \cdot p^2 - k_p \cdot p - q_T \cdot T^2 - k_T \cdot T. \tag{5.9}$$

5.1.7 Compensated Rolling Radius Performance Evaluation

As described in Section 1.2 the compensated rolling radius should be independent of vehicle velocity, tire pressure, tire temperature, load and applied torque. It should mostly depend on the tread depth. Since tread depth is strictly decreasing over time and it is decreasing slowly, the compensated rolling radius should strictly decrease and have low variance. The performance of the compensation models are evaluated by two metrics. Firstly the change in compensated rolling radius over time. If it is constant or increasing over time, it cannot be used to estimate tread wear. Meaning that the compensated rolling radius is unusable. The relationship between change in nominal rolling radius and tread wear is unknown. This means that even though tread depth measurements are available, they cannot be used to evaluate change in compensated rolling radius. This all means that any compensated rolling radius signal that decreases over time is approved while any compensated rolling radius signal that increases or is constant is not approved. The compensated rolling radius signal will have the initial tire growth phenomen, described in Section 5.1.3, however after 500,000 s this is assumed to no longer have an impact. This means that the compensated rolling radius should be decreasing after 500,000 s. The second metric of the signal is the standard deviation. Given the slow nature of tread wear, the theoretical nominal rolling radius should have almost no variance. This means that the compensated rolling radius signal should have as low standard deviation as possible.

The standard deviation of the compensated rolling radius are calculated after medians have been applied. It is done by firstly using the MATLAB function *fit* to fit a curve to the medians of the compensated rolling radius. This is done on the data after 500,000 s to avoid the initial tire growth effects. Then the standard deviation is calculated on the distance from the signal to the fitted line. This method for calculating standard deviation is used in all further sections.

5.1.8 Validation Method

This section describes two methods for validation of the compensation model. Both validation methods are performed on the test cases described in Section 3.

5.1.8.1 Self-validation

As mentioned earlier an approach where the validation is performed on the training data would yield a result showing that the *Quadratic* model performs equally good or likely even slightly better than the *V-Quadratic* model due to the higher degree of freedom. Validating on the training data, i.e., self-validation, can still be relevant in comparison to other validation methods. It can however not be used alone to determine the performance of a model.

5.1.8.2 K-Fold Cross Validation

One way to validate the different compensation models and compare performances, is to use k-fold cross validation. K-fold cross validation is when one divides the available data set into k number of folds. And then let all but one fold be used for training and the remaining fold is used for validation. This can be iterated by changing which fold is excluded until all combinations have been covered. In this thesis 5 folds are used. One concern in this case is that a tire deteriorates over time. Meaning that the tire acts differently when it is new compared to when it is almost worn out. The most notable effects of this concern is the initial tire growth. For this reason it is excluded from the data set.

5.2 Results

In this Section the results from the rolling radius compensations are presented.

5.2.1 Rolling Radius Dependency on External Factors

Rolling radius has as previously discussed a dependency of different external factors. Here are the dependencies in rolling radius due to velocity, tire pressure and tire temperature investigated. When investigating the radius dependency with respect to the velocity the result visualized in Figure 5.6, shows how an increasing velocity yields an increasing pre-compensated rolling radius, r_{pc}. The medians are applied to the pre-compensated rolling radius in segments of 5 km/h. Both a linear and a quadratic line have been fitted to the data and both seems to fit the data well. The quadratic model seems to fit the median values slightly better in this data set. Which indicates that the there might be a stronger quadratic relationship, rather than a linear one. This does however not necessarily mean that the relationship is in fact quadratic, it could be a coincidence. Further investigations whether a linear or quadratic compensation model works better is necessary.

Some noisy measurements are obtained for the higher velocities since, when driving at velocities over approximately 140 km/h, the amount of data points is heavily decreased compared to the rest of the velocities, resulting in more inaccurate results when calculating the median radius for these velocities. After applying the linear compensation one can see how the undesired behavior of the radius due to changes in the velocity is now reduced when plotting the compensated rolling radius, $r_{comp,l}$, as a function of velocity as can be seen in Figure 5.6. The increasing radius at higher velocities are still present but this is, as previously discussed, likely due to the lack of data points at higher velocities, which increases the impact of signal noise.

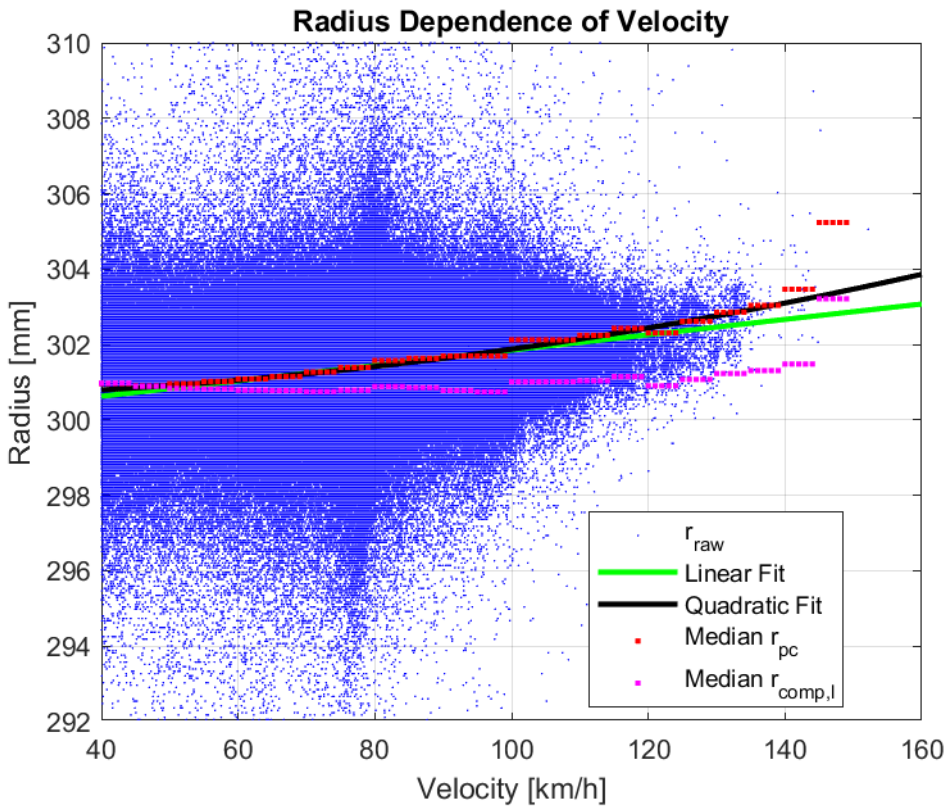

Figure 5.6: Medians of the pre-compensated rolling radius as a function of velocity as well as the linear compensated rolling radius as a function of velocity. For a FL tire on Test Case 4.

As for the pressure, the pre-compensated rolling radius, r_{pc}, has a dependence with change tire pressure. This relation is illustrated in Figure 5.7, where one can see that an increasing tire pressure yields an increasing pre-compensated rolling radius. Also here the medians are calculated for pressure spans of 5 kPa as for the velocity above. These calculated medians yield a very linear behavior and both a linear and a quadratic fit have been applied to the model with not to much of a difference between them. Indicating that the relationship might be linear.

After applying the linear compensation with the relation between the linear compensated rolling radius, $r_{comp,l}$, and tire pressure can be seen in Figure 5.7. The compensated rolling radius dependency due to increasing tire pressure is now compensated for and this relation between increasing tire pressure and increasing rolling radius is reduced.

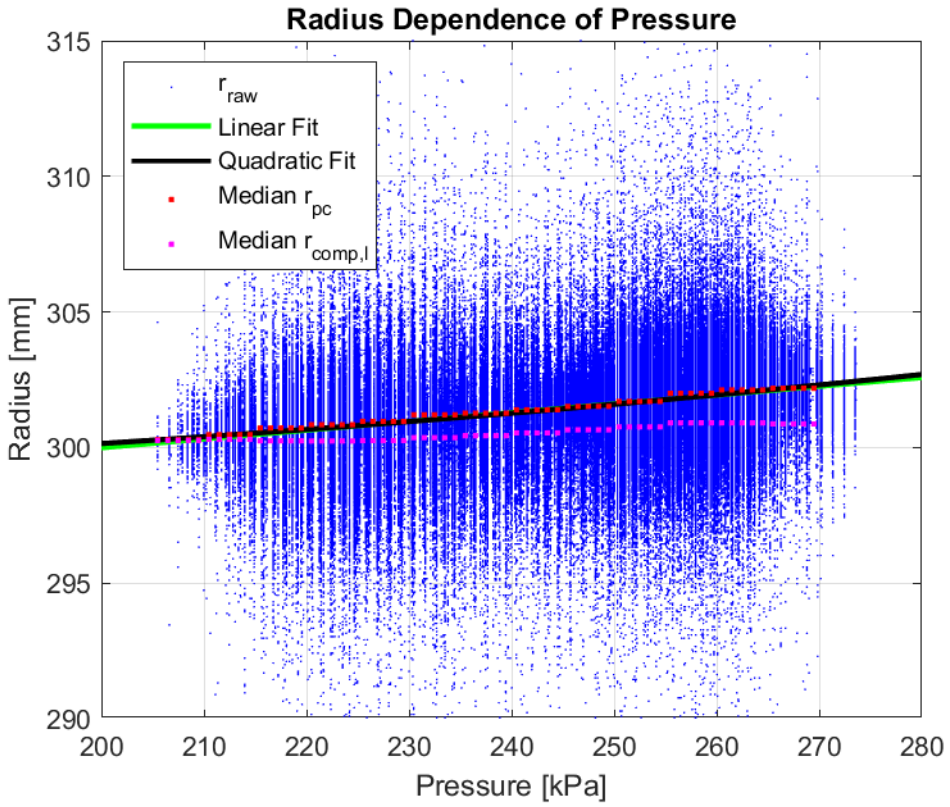

Figure 5.7: Medians of the pre-compensated rolling radius as a function of tire pressure as well as the linear compensated rolling radius as a function of tire pressure. For a FL tire on Test Case 4.

Lastly, the tire temperature, which is the third external dependency factor, is treated. In Figure 5.8 one can see the impact of increasing tire temperature on the pre-compensated rolling radius, r_{pc}. An increasing tire temperature does not have an equally large impact on the pre-compensated rolling radius as the velocity and the tire pressure previously discussed. Although, an relation between increasing tire temperature and increasing pre-compensated rolling radius can be observed.

The tire temperature dependency are linearly compensated for and when doing this the result in Figure 5.8 is obtained. Here, one can see how the dependency between linear compensated rolling radius, $r_{comp,l}$, and increasing tire temperature is compensated for.

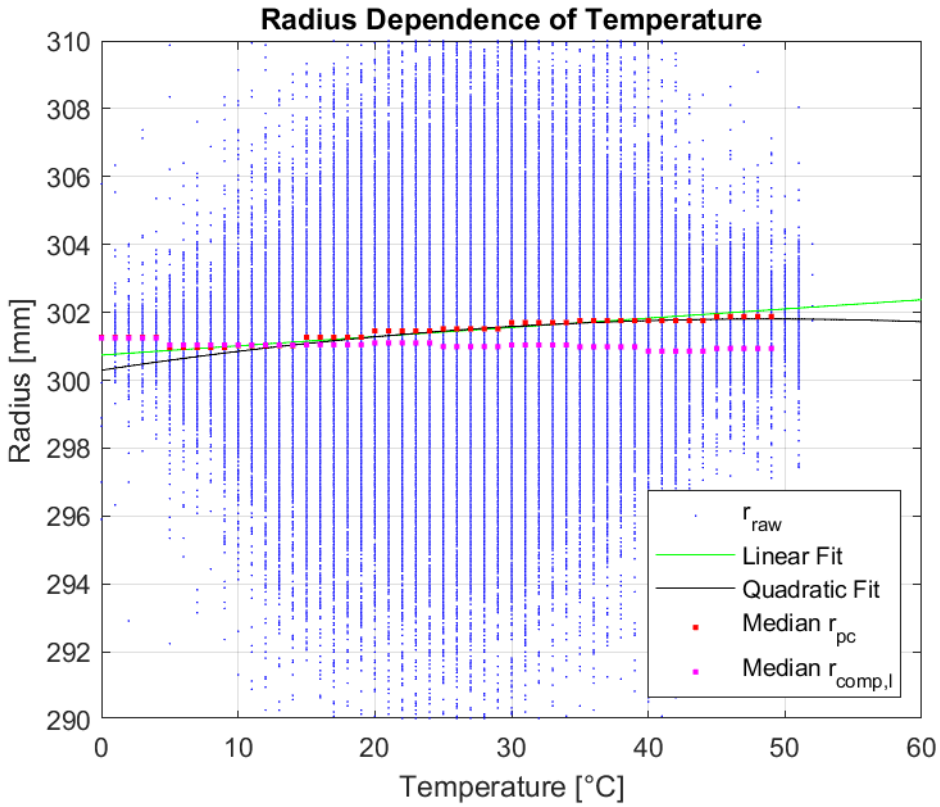

Figure 5.8: Medians of the pre-compensated rolling radius as a function of tire temperature as well as the linear compensated rolling radius as a function of tire temperature. For a FL tire on Test Case 4.

Table 5.1 shows the R^2 values of the fitted lines in Figure 5.6-5.8. R^2 describes how much of the noise in the data that can be explained by the model (fitted line) in relation to the entire signal noise. The quadratic fits should in general always result in a higher R^2 value. Whats relevant is how much better the quadratic fits are, in comparison to the linear fits. If the linear and quadratic fits have almost the same R^2 values, the relationship between pre-compensated rolling radius and the corresponding variable is most likely linear. If the R^2 of the quadratic fit is significantly higher, this would indicate a more quadratic relationship than a linear one. For the pressure plot there is almost no difference between the R^2 values, meaning that the relationship between pre-compensated rolling radius and tire pressure is linear. The temperature plot has a slightly higher R^2 for the quadratic model meaning that there is a slight advantage of using a quadratic model. The Velocity plot has the biggest difference in R^2 between linear and quadratic fitted lines. This means that is a more quadratic than linear relationship between rolling radius and vehicle velocity. The R^2 values also indicate that a majority of the variance in the signal is not explained by any of the variables, v, p, T.

Table 5.1: This table shows the R^2 of the fitted lines in Figure 5.6-5.8.

	Linear Fit	Quadratic Fit
Velocity Plot	5.12%	5.22%
Pressure Plot	12.39%	12.4%
Temperature Plot	1.96%	2.06%

5.2.2 Linear Compensation Results

The resulting compensated radii using the iterative compensation procedure is shown in Figure 5.9 for a FL tire and in Figure 5.10 for a RL tire. Medians over 10,000 s have been applied to decrease

noise. Trend lines have been fitted to the set of data after 500,000 seconds (139 h). The different heights that the curves are on is insignificant, the signal is evaluated by the absolute decrease of the fitted line and the noise of the rolling radius signal. When comparing both figures one can see that the yellow compensation model yields an undesired behavior of the rolling radius on the rear tire, where the rolling radius is increasing with time. It can be seen that both the front tire and the rear tire get a more accurate estimation of the radius decrease due to tread wear over time when including the temperature in the model. Finally, this results in that the compensation method to move forward with is the compensation model compensating for velocity, tire pressure and tire temperature which also includes the tread wear in the regression model.

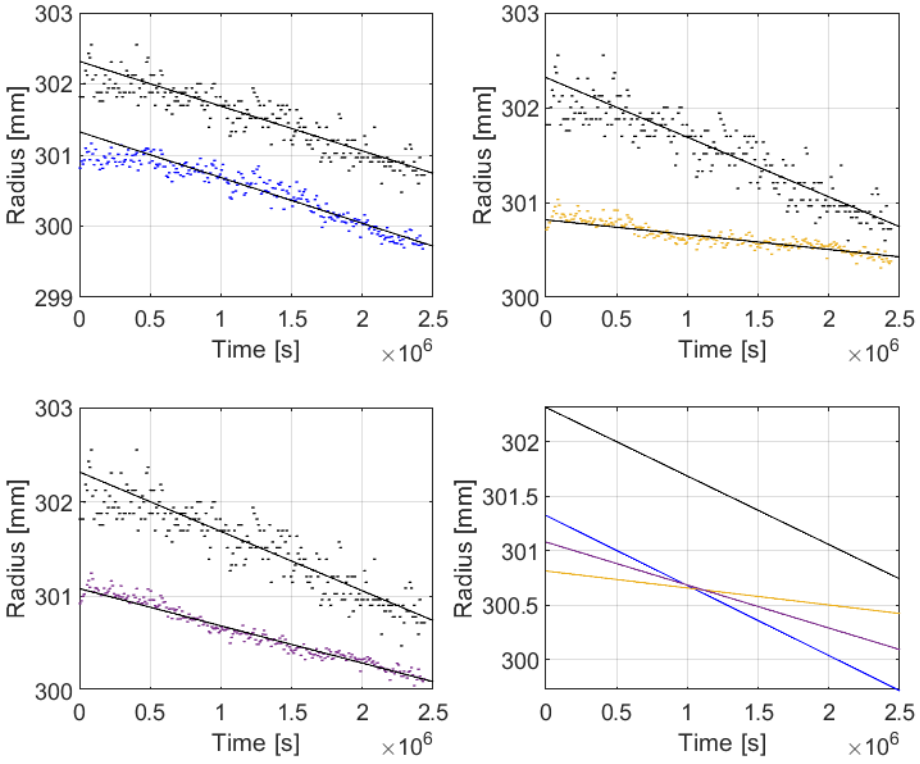

Figure 5.9: This figure illustrates the different linear rolling radius compensations. The top left figure shows the pre-compensated rolling radius signal in black compared to the velocity compensated rolling radius signal in blue. The top right figure shows the pre-compensated rolling radius signal in black compared to the tire pressure and velocity compensated rolling radius signal, where the tread wear is included in the regression model, in yellow. The bottom left figure shows the pre-compensated rolling radius signal in black compared to the tire temperature, tire pressure and velocity compensated rolling radius signal, where the tread wear is included in the regression model, in purple. The bottom right figure shows the decrease in rolling radius for the three compensations. All for a FL tire on Test Case 4.

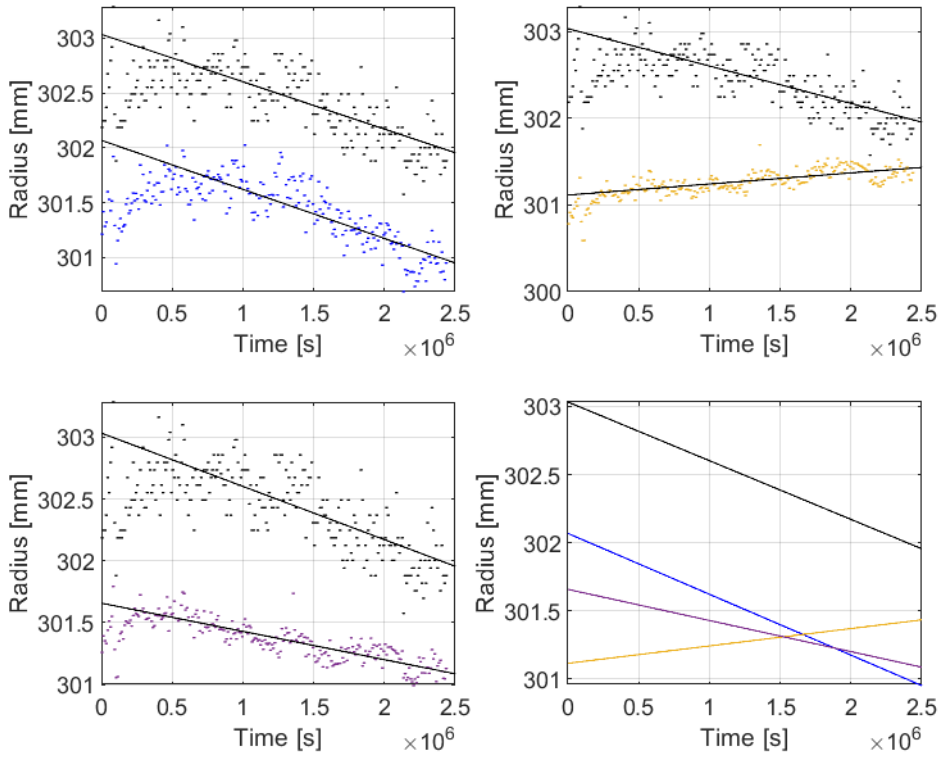

Figure 5.10: This figure illustrates the different linear rolling radius compensations. The top left figure shows the pre-compensated rolling radius signal in black compared to the velocity compensated rolling radius signal in blue. The top right figure shows the pre-compensated rolling radius signal in black compared to the tire pressure and velocity compensated rolling radius signal, where the tread wear is included in the regression model, in yellow. The bottom left figure shows the pre-compensated rolling radius signal in black compared to the tire temperature, tire pressure and velocity compensated rolling radius signal, where the tread wear is included in the regression model, in purple. The bottom right figure shows the decrease in rolling radius for the three compensations. All for a RL tire on Test Case 4.

5.2.3 Quadratic Compensation Results

After deciding which of the linear compensation models that resulted in the most efficient compensated rolling radius this method was compared to the two different quadratic models described in Section 5.1.6. In Figure 5.11 one can see a comparison between the different compensation methods; the pre-compensated radius signal, the *Linear* compensation, the *V-Quadratic* compensation and the *Quadratic* compensation. As previously explained there is no significance in the height that the curves are on. The evaluations are done exclusively on the gradients of the slopes and the noise of the rolling radius signal. The result from this is that it is hard to tell whether there is any improvements with using a quadratic compensation method by just plotting the change in radius over time. One result that can be concluded from Figure 5.11 is that the *Quadratic* compensation yield a significantly steeper gradient than the *Linear* and *V-Quadratic* compensations and it even has a steeper gradient than the pre-compensated radius. Due to the slight diffusion of the tire pressure, seen in Figure 3.4, over time in Test Case 4, the gradient after applying compensation is expected to have a flatter gradient than the pre-compensated one. To decide whether to use the *Linear* or any of the quadratic compensation models, a more in depth investigation regarding the standard deviations is needed.

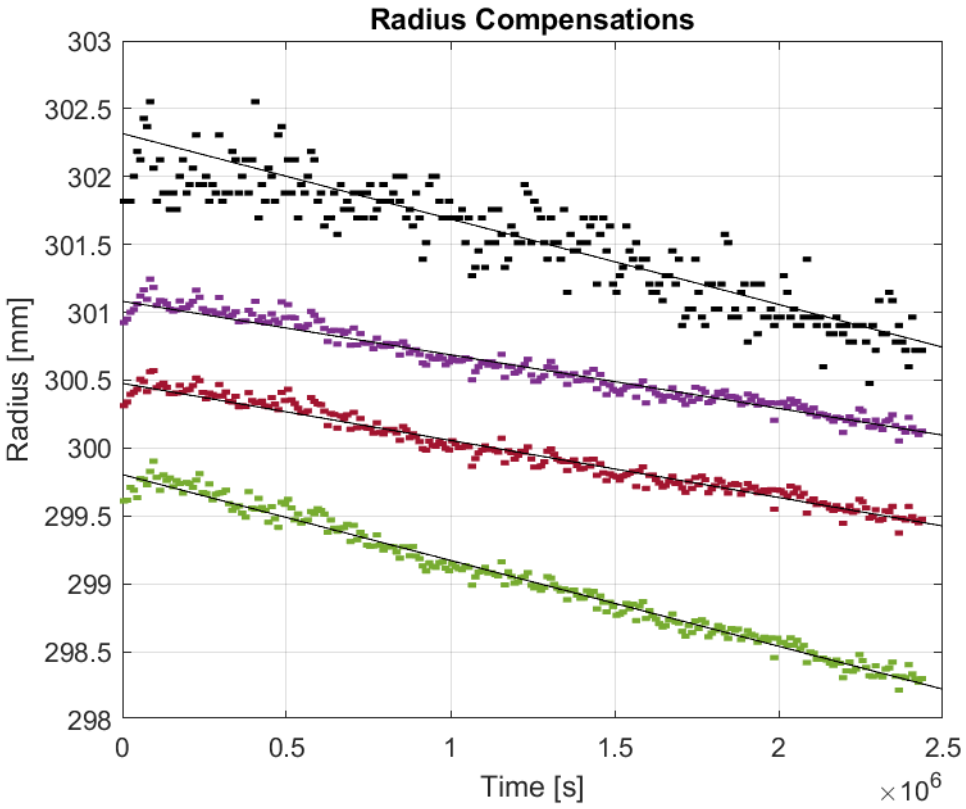

Figure 5.11: This figure illustrates the pre-compensated rolling radius signal in black, the *Linear* compensation in purple, the *V-Quadratic* compensation in red and the *Quadratic* compensation in green. All for a FL tire on Test Case 4.

5.2.4 Validation

This section presents the results from validating the compensation models presented above, with the intent of finding the model that performs best. This is done by evaluating the models through both self-validation and k-fold validation.

5.2.4.1 Self-Validation Results

This self-validation was performed on all four test cases presented in Section 3.1. The results for the standard deviations, using the self-validation approach, are shown in Table 5.2.

Table 5.2: This table displays the standard deviation between the three models: Linear, *V-Quadratic* and *Quadratic* for all test cases.

Standard Deviations					
Test Case	Model	FL [mm]	FR [mm]	RL [mm]	RR [mm]
Test Case 1	*Linear*	0.077	0.071	0.111	0.085
	V-Quadratic	0.072	0.063	0.104	0.078
	Quadratic	0.073	0.064	0.104	0.078
Test Case 2	*Linear*	0.074	0.082	0.085	0.095
	V-Quadratic	0.065	0.073	0.075	0.089
	Quadratic	0.065	0.072	0.074	0.086
Test Case 3	*Linear*	0.112	0.108	0.126	0.124
	V-Quadratic	0.109	0.106	0.123	0.121
	Quadratic	0.109	0.104	0.122	0.119
Test Case 4	*Linear*	0.053	0.060	0.083	0.086
	V-Quadratic	0.052	0.060	0.082	0.086
	Quadratic	0.050	0.060	0.080	0.082

To evaluate the standard deviations of the *V-Quadratic* model and the *Quadratic* model they are compared with the *Linear* model by comparing the change in standard deviation. This change in standard deviation is calculated according to (5.10)

$$\sigma_{diff} = \frac{\sigma}{\sigma_{Linear}} - 1, \tag{5.10}$$

where σ is either $\sigma_{V-Quadratic}$ or $\sigma_{Quadratic}$. A negative percentage value relates to a decrease in standard deviation compared to the *Linear* model. These values can be seen in Table 5.3.

Table 5.3: This table displays the change in standard deviation in percent when comparing the *Linear* model to the *V-Quadratic* model and the *Quadratic* model.

Standard Deviations					
Test Case	Model	FL	FR	RL	RR
Test Case 1	*V-Quadratic*	-7.24%	-10.96%	-6.40%	-8.13%
	Quadratic	-6.21%	-10.67%	-6.13%	-8.01%
Test Case 2	*V-Quadratic*	-11.56%	-11.48%	-11.63%	-6.43%
	Quadratic	-12.24%	-11.72%	-13.51%	-9.27%
Test Case 3	*V-Quadratic*	-2.24%	-2.22%	-2.07%	-1.70%
	Quadratic	-2.51%	-3.52%	-2.71%	-3.56%
Test Case 4	*V-Quadratic*	-0.76%	-0.83%	-0.36%	-0.35%
	Quadratic	-5.14%	-1.50%	-3.63%	-4.66%

Using this self-validation approach shows that the *V-Quadratic* model and the *Quadratic* model performs almost equally good if compared to the *Linear* model.

5.2.4.2 K-fold

The results from the k-fold validation are presented in Table 5.4 where the mean values for all test cases are presented. All the standard deviations for each fold and test case can be found in Table 10.1 - 10.4 in Appendix.

Table 5.4: Mean values of the standard deviations for the *Linear*, *V-Quadratic* and *Quadratic* compensation models for each tire and validated on each data fold.

Standard Deviations												
	Linear				*V-Quadratic*				*Quadratic*			
Test case	FL	FR	RL	RR	FL	FR	RL	RR	FL	FR	RL	RR
Test Case 1	0.063	0.064	0.089	0.077	0.059	0.059	0.084	0.073	0.061	0.063	0.085	0.076
Test Case 2	0.066	0.076	0.081	0.089	0.06	0.071	0.071	0.084	0.067	0.075	0.069	0.081
Test Case 3	0.086	0.085	0.095	0.098	0.083	0.084	0.094	0.097	0.086	0.086	0.098	0.104
Test Case 4	0.042	0.048	0.069	0.069	0.043	0.049	0.07	0.071	0.044	0.049	0.069	0.07

Table 5.5: This table displays the change in average standard deviation over all 5 folds when comparing the *Linear* model to the *V-Quadratic* model and the *Quadratic* model.

Standard Deviations					
Test Case	Model	FL	FR	RL	RR
Test Case 1	*V-Quadratic*	-6.03 %	-8.13 %	-5.8 %	-6.03 %
	Quadratic	-3.76 %	-1.86 %	-5.25 %	-1.26 %
Test Case 2	*V-Quadratic*	-9.42 %	-6.87 %	-12.04 %	-6.42 %
	Quadratic	1.49 %	-0.98 %	-14.14 %	-9.32 %
Test Case 3	*V-Quadratic*	-3.37 %	-1.33 %	-1 %	-0.45 %
	Quadratic	-0.25 %	0.52 %	3.28 %	6.63 %
Test Case 4	*V-Quadratic*	2.19 %	0.95 %	1.62 %	2.03 %
	Quadratic	2.65 %	1.96 %	0.52 %	1.07 %

To determine which of the compensation models performed the best; the average result of the k-fold validation of the *V-Quadratic* and *Quadratic* model is compared with the average result for the *Linear* model. However, for Case 4 there is an increase in standard deviation for both quadratic compensation models when comparing to the *Linear* model. It also, overall, shows that the *V-Quadratic* model performs better than the *Quadratic* model. This could mean that the quadratic terms for the tire pressure and tire temperature results in some overfitting; which decreases the performance gains compared to the *V-Quadratic* model. The *V-Quadratic* model do however, from an overall perspective, perform best when comparing the models.

5.3 Discussion

The linear regression model in (5.4) includes v, p, T and l_{TD}. The inclusion of v, p and T were motivated by physical relationships as discussed in Section 5.1.4. l_{TD} was added to the model because it was found that without it, the compensation model quickly "overcompensates". Overcompensation means that the compensated rolling radius signal becomes constant over time. Since the purpose of the compensation is to achieve a compensated rolling radius signal that can be used to evaluate tread wear over time, this overcompensation is undesirable. This overcompensation is especially clear when using a pressure only compensation model. An issue with this model is that the pressure, unlike the velocity can have trends over time, see Section 3.1. E.g., in Test Case 4 where the pressure decreases over time, see Figure 3.4. This means that since the pressure is decreasing over time, the pre-compensated rolling radius will also decrease. This means that a regression model on the form

$$\hat{r}_p = k_p \cdot p + m, \tag{5.11}$$

where $\hat{r}_p$ is the model fitted to data. This regression model has corresponding compensation model on the form

$$r_{comp,p} = r_{pc} - k_p \cdot p, \tag{5.12}$$

where $r_{comp,p}$ is the pressure compensated rolling radius. This regression and compensation model will confuse decrease in pre-compensated rolling radius due to tread wear with decrease in pre-compensated rolling radius due to pressure drop. So, after pressure compensation, the signal will be overcompensated, and the rolling radius decrease due to tread wear will disappear. Since the aim of the compensation is to achieve a signal that can be used to estimate tread wear, a constant rolling radius signal is useless. The resulting compensation is shown in Figure 5.12, and it is clear that the signal has been overcompensated since it has zero slope after the initial tire growth.

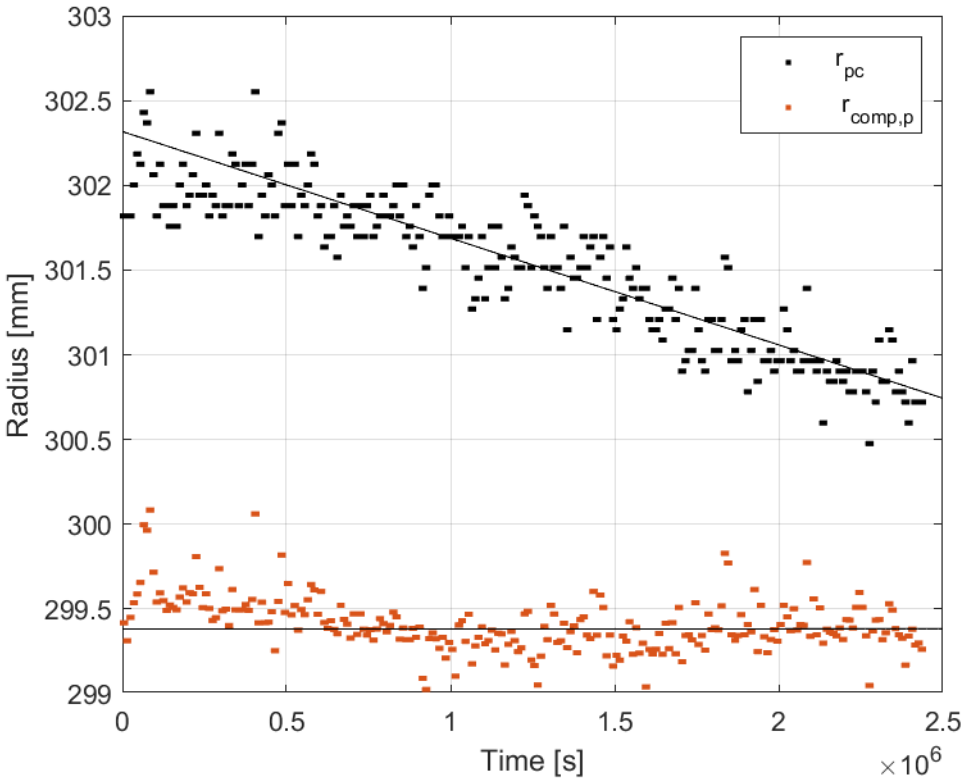

Figure 5.12: This figure shows the pre-compensated rolling radius signal with medians, r_{pc}, and the pressure compensated rolling radius with medians, $r_{comp,p}$. The signals also have fitted lines, that has been fitted on the data after 500,000 s.

To avoid this overcompensation, the effects of tread wear over time needs to be included in the regression model so that the signal does not get overcompensated. One solution could be to look at shorter time intervals when the change in tread wear is negligible, however after testing it was found that even intervals of 100,000 s (5% of the test case) resulted in overcompensation. Even shorter intervals had issues with noise and outliers having a too large of an effect. Another method would be to assume that the tread wear decreases linearly with time, and include the time vector in the linear least squares regression. However, tread wear is quite dependent on driving style and other factors meaning that it might not be linear over time. As to not introduce any biases in how the tread wear decreases over time, the actual, measured tread depth can be used. By including this, one can determine if this method for compensating the pre-compensated rolling radius actually works, with no assumption of how the tread wears over time. This is the reason for including l_{TD} and k_{TD} in the regression model $\hat{r}_l$ in (5.4).

Tire pressure, tire temperature and velocity are somewhat correlated. E.g., the tires heat up while driving due to friction, which increases tire temperature and tire pressure. Since the variables have some correlation, this means that if one were to calculate the dependency factors independently from each other; and then apply them all in the compensation, there is a risk that the same rolling radius phenomenon is compensated several times. Therefore the dependency factors are calculated simultaneously.

From Section 5.2.4.1 one might at first glance believe that the *Quadratic* model is the best of the three compensation models. However, as previously discussed self-validation is a poor method for evaluating a models performance. By instead using k-fold cross validation the models can be evaluated in a more credible way. From Section 5.2.4.2 it is clear that the *V-Quadratic* model is better than the *Quadratic* and *Linear* model. This means that the final compensation model will use a regression model on the form

$$\hat{r}_{vq} = q_v \cdot v^2 + k_v \cdot v + k_p \cdot p + k_T \cdot T + k_{TD} \cdot l_{TD} + m, \tag{5.13}$$

with medians applied to segments of 10000 s. Subtracting the dependency factors obtained from times the corresponding variable from the pre-compensated rolling radius gives the V-Quadratic compensation model is on the form

$$r_{comp,vq} = r_{pc} - q_v \cdot v^2 - k_v \cdot v - k_p \cdot p - k_T \cdot T. \tag{5.14}$$

The result from applying this compensation model on Test Case 2 can be seen in Figure 5.13 and in Table 5.6. There is a significant decrease in signal noise, a decrease of around 75% for each tire.

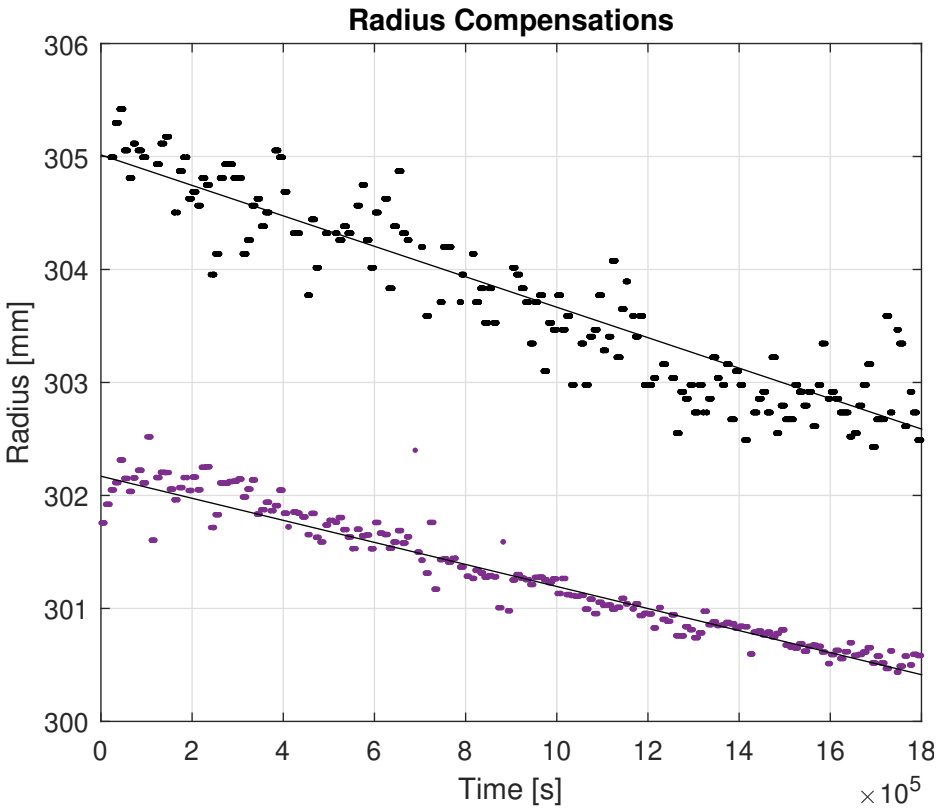

Figure 5.13: This figure shows the performance of the final model on the FL tire on Test Case 2.

Table 5.6: This table compares the standard deviation of the pre-compensated rolling radius signal and the compensated rolling radius signal using the *V-Quadratic* model.

	FL	FR	RL	RR
Pre-compensated	0.3125	0.3126	0.3414	0.3233
V-Quadratic	0.068	0.078	0.073	0.085
Decrease	-78.24%	-75.05%	-78.62%	-73.71%

The mean of the R^2 values for all test cases are shown in Table 5.7. It is calculated on the signal prior to application of medians. It shows that only 9-18% of all noise in the rolling radius signal can be described by the regression model. This means that 80% of the noise remains in the signal after compensation. This remaining noise is assumed to be Gaussian noise or so called white noise. I.e., normally distributed noise. This is the main purpose of the medians, to reduce "random noise". If there is an underlying bias, e.g., from a change in pressure, this will show even after the median segments have been applied. Since the standard deviation is significantly lower after compensation, it is clear that most of the bias has been removed.

Table 5.7: This table shows the mean of the R^2 values for each tire from the regression model calculations on all test cases.

Test Case	FL	FR	RL	RR
Test Case 1	10,26 %	9,64 %	10,18 %	9,12 %
Test Case 2	17,64 %	15,57 %	14,52 %	13,47 %
Test Case 3	13,26 %	11,35 %	10,35 %	9,94 %
Test Case 4	12,46 %	11,85 %	10,03 %	9,87 %

The effectiveness of the *V-Quadratic* compensation method is even clearer on a test case with a tire pressure drop, such as in Test Case 3. See Figure 3.3. The final compensation model applied on Test Case 3 is shown in Figure 5.14. The figure illustrates how the drop in tire pressure results in a drop in the pre-compensated rolling radius signal as well. This drop is successfully removed after the compensation model, resulting in a straighter and less noisy signal. There is a significant increase in noise around the tire pressure drop, this is because of the enhancement of the tire pressure signal, described in section 5.1.2, gives poor values around the tire pressure drop. Meaning that this noise can be neglected. The remaining part of the signal has little noise and no rolling radius drop at the pressure drop.

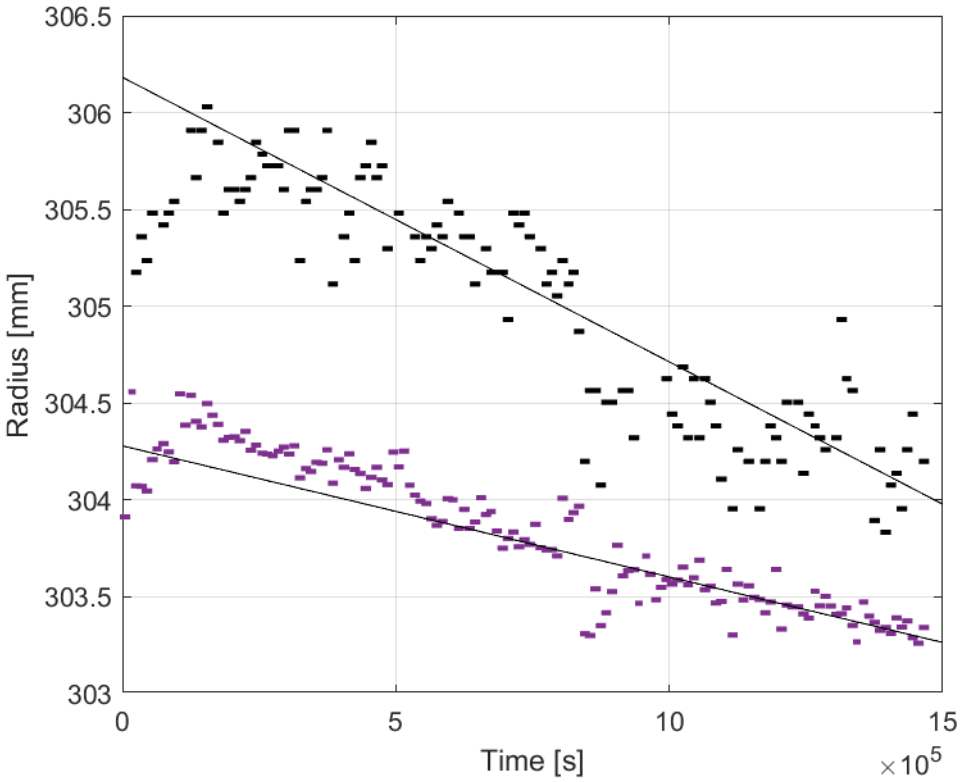

Figure 5.14: This figure shows the pre-compensated signal and the fully compensated signal for Test Case 3.

6 Adaptive Rolling Radius Compensation

As previously discussed the *V-Quadratic* model yields the best compensation performance and therefore this model is used in further investigations. After choosing the compensation method, this method can be used to investigate whether there is a need for adaptive compensation factors between different vehicles or not. As described in Section 1.2 there is no way for a vehicle to detect which tire a vehicle has equipped at a given time. Since tires wear out and are replaced, one can also not assume that the vehicle has the tire that the OEM equipped it with when the vehicle was manufactured. Different tires have different material properties, tread patterns and tread depths. This means that they will behave differently. The question is if the compensation method needs to adapt to the current tire set or if it can use the same compensation model for all tire sets on a given vehicle. This is investigated by comparing the performance of the individually trained models described in the previous chapter with models that are not individually adapted. The k-fold approach, previously mentioned, is used as a baseline for the performance of the individually adaptive compensation.

6.1 Method

The need for tire adaptivity can be investigated using different approaches. This thesis will investigate it by comparing the performance of an adaptive, individually trained compensation models, from Chapter 5, with nonadaptive compensation models. In a final in-vehicle product, an adaptive compensation model would need to learn and adapt the compensation dependency factors online and recalculate them every time the car is equipped with new tires. A nonadaptive compensation model could always use predefined dependency factors that are fixed for that car type, this would reduce the complexity of a final, online compensation model. The question is how this nonadaptivity would affect the performance of the compensation model. This thesis investigates this question by comparing the results from the k-fold validation in the previous chapter to two nonadaptive models that have been pretrained in different ways.

The first training method is denoted as *Single Training*. It is trained on a single test case and then evaluated on the other test cases. This approach is tested on all four vehicles in the test data, meaning that there are twelve combinations. This training method is meant to emulate the performance the system would get, if OEM trained the model once on a single tire set.

The second training method includes training the regression model on several test cases and calculating an average value for each dependency factor and then using these values for validating each vehicle separately, this method will be denoted as *Multiple Training* in future sections. This method is meant to emulate the performance the system would get, if OEM trained the model on several different tire sets and took the averages of the compensation factors.

6.2 Result

This section presents the results of the adaptivity investigation.

6.2.1 Single Training

In Table 6.1 - 6.4 the standard deviations from using the *Single Training* approach can be seen. Each table presents the standard deviation achieved when using the *V-Quadratic* model on a given test case, when it has been trained on the other available test cases. The results from the k-fold validation is included as the result of training and validating the model on the same test case. From the tables it is clear that the performance varies a lot depending on which test case the model has been trained on. This variance in how well the model performed can be seen as unreliability, which is not a desired result. Meaning that this *Single Training* method is a poor alternative to an adaptive compensation model.

Table 6.1: Standard deviations for *Single Training* when validating on Test Case 1 together with how much the standard deviation is increased compared to the k-fold validation.

Standard Deviations				
Training Test Case	FL	FR	RL	RR
k-fold	0.059	0.059	0.084	0.073
Test Case 2	0.081	0.066	0.105	0.079
Test Case 3	0.098	0.094	0.126	0.105
Test Case 4	0.075	0.076	0.111	0.085
Increase				
Test Case 2	37.63 %	12.2 %	24.76 %	7.95 %
Test Case 3	66.61 %	59.83 %	49.64 %	43.15 %
Test Case 4	26.27 %	28.81 %	32.14 %	16.3 %

Table 6.2: Standard deviations for *Single Training* when validating on Test Case 2 together with how much the standard deviation is increased compared to the k-fold validation.

Standard Deviations				
Training Test Case	FL	FR	RL	RR
k-fold	0.06	0.071	0.071	0.084
Test Case 1	0.079	0.078	0.077	0.092
Test Case 3	0.091	0.1	0.106	0.111
Test Case 4	0.089	0.08	0.08	0.09
Increase				
Test Case 1	32.33 %	9.72 %	7.75 %	9.05 %
Test Case 3	51.17 %	40.85 %	49.15 %	32.38 %
Test Case 4	48.17 %	12.54 %	12.96 %	7.62 %

Table 6.3: Standard deviations for *Single Training* when validating on Test Case 3 together with how much the standard deviation is increased compared to the k-fold validation.

Standard Deviations				
Training Test Case	FL	FR	RL	RR
k-fold	0.083	0.084	0.094	0.097
Case 1	0.118	0.145	0.133	0.149
Case 2	0.135	0.124	0.132	0.132
Case 4	0.119	0.113	0.14	0.168
Increase				
Case 1	42.53 %	72.26 %	41.17 %	53.51 %
Case 2	62.41 %	47.02 %	40.11 %	36.49 %
Case 4	43.49 %	34.4 %	48.51 %	72.78 %

Table 6.4: Standard deviations for *Single Training* when validating on Test Case 4 together with how much the standard deviation is increased compared to the k-fold validation.

Standard Deviations				
Training Test Case	FL	FR	RL	RR
k-fold	0.043	0.049	0.07	0.071
Test Case 1	0.056	0.071	0.085	0.086
Test Case 2	0.052	0.069	0.084	0.091
Test Case 3	0.053	0.066	0.083	0.093
Increase				
Test Case 1	30.23 %	45.1 %	21.29 %	21.13 %
Test Case 2	20.93 %	41.63 %	20 %	27.46 %
Test Case 3	23.26 %	34.08 %	18.29 %	31.41 %

6.2.2 Multiple Training

The compensation model can be evaluated on two premises. The first is the amount of noise of the signal, and the second is the gradient of the decrease over time. The results of the *Multiple Training* regarding signal noise is presented in Table 6.7. Table 6.6 include the results from the k-fold validation from Chapter 5, it is used as reference for the adaptive model. The standard deviation of the pre-compensated signal is shown in Table 6.5. The change in standard deviation when comparing the k-fold results with the *Multiple Training* approach is presented in Table 6.8. In Figure 6.1 and Figure 6.2 the results after applying the *Multiple Training* is compared to the pre-compensated rolling radius signal and also the *V-Quadratic* compensation.

Table 6.5: This table shows the standard deviation for each test case for the pre-compensated signal.

Test Case	FL	FR	RL	RR
Test Case 1	0.287	0.279	0.328	0.307
Test Case 2	0.313	0.313	0.341	0.323
Test Case 3	0.256	0.246	0.308	0.305
Test Case 4	0.168	0.157	0.202	0.188

Table 6.6: This table shows the standard deviation for each test case using k-fold.

Test Case	FL	FR	RL	RR
Test Case 1	0.059	0.059	0.084	0.073
Test Case 2	0.06	0.071	0.071	0.084
Test Case 3	0.083	0.084	0.094	0.097
Test Case 4	0.043	0.049	0.07	0.071

Table 6.7: This table shows the standard deviation for each test case using the model trained on all vehicles.

Validation Test Case	FL	FR	RL	RR
Test Case 1	0.083	0.074	0.113	0.086
Test Case 2	0.067	0.082	0.091	0.101
Test Case 3	0.094	0.097	0.098	0.103
Test Case 4	0.053	0.067	0.086	0.092

Table 6.8: This table shows the change in standard deviation for each test case and tire when comparing an adaptive compensation model to a multiple training compensation model.

Test Case	FL	FR	RL	RR
Test Case 1	40.16 %	26.08 %	34.2 %	18.15 %
Test Case 2	12.13 %	16.1 %	27.91 %	20.62 %
Test Case 3	13.09 %	15.14 %	3.82 %	5.96 %
Test Case 4	22.13 %	36.85 %	22.46 %	29.97%

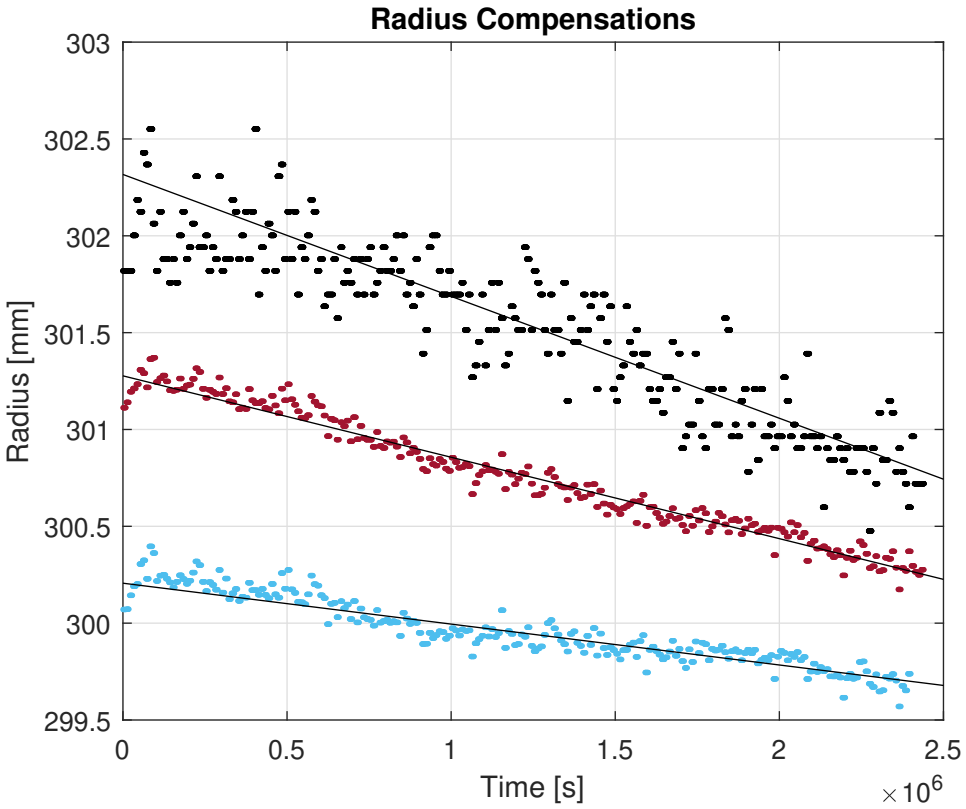

Figure 6.1: This figure illustrates the pre-compensated radius signal in black, the *V-Quadratic* compensation in red and the *Multiple Training* in blue. All for a FL tire on Test Case 4.

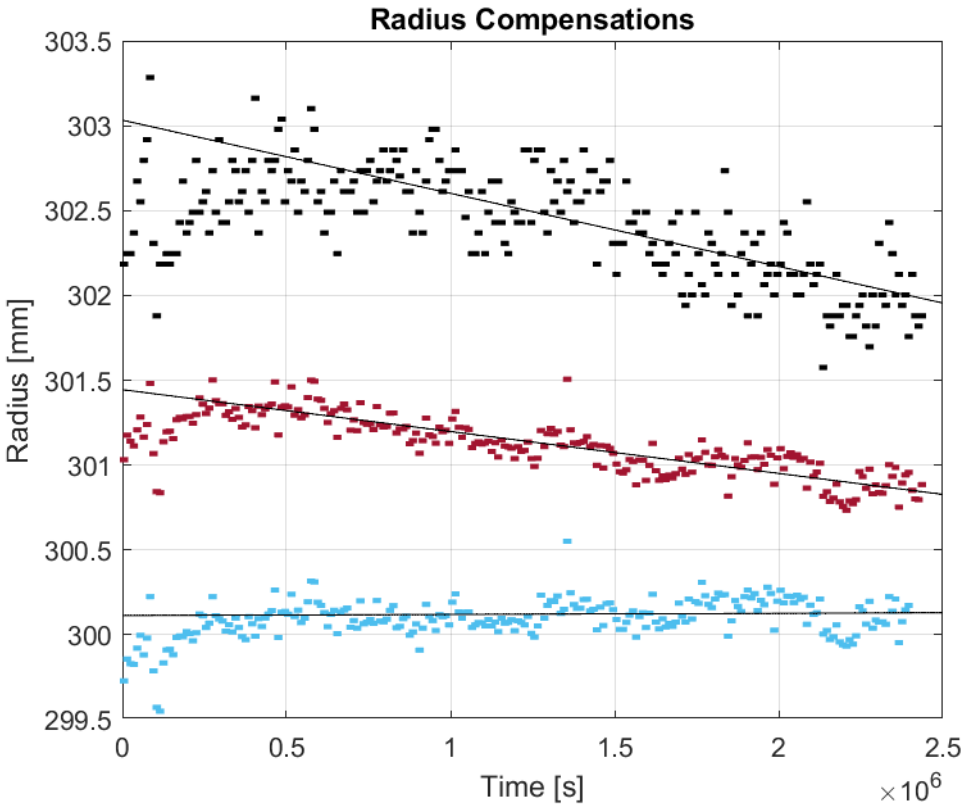

Figure 6.2: This figure illustrates the pre-compensated radius signal in black, the *V-Quadratic* compensation in red and the *Multiple Training* in blue. All for a RL tire on Test Case 4.

6.3 Discussion

Evaluating the need of adaptivity between tire sets have been done using the approaches called *Single Training* and *Multiple Training*. When evaluating adaptivity using the *Single Training* the results shows a large variance in consistency depending on which vehicle the model was trained on. If comparing the standard deviations to the ones obtained using the individually adaptive k-fold model, in Tables 6.1-6.4, this shows an increase for all possible training/validation combinations. This is an expected result, due to the fact that using compensation factors, calculated from one vehicle, on another vehicle would obviously yield a worse result compared to if instead calculating them on the same vehicle as for the k-fold model. It is clear that when validating on Test Case 3, which is the test case with the large tire pressure drop, one can see a more significant increase in standard deviation compared to the other test cases. This yields an increase of around 50% for all tires whereas when validating on the other test cases this increase is around 30% for all tires.

The second approach to investigate the need of adaptivity is the *Multiple Training*. Table 6.8 shows that there is an increase when going from an individually adaptive model to the nonadaptive *Multiple Training* model. However, compared to the pre-compensated signal the *Multiple Training* model is still far less noisy. This would indicate that depending on the requirements of a final, in-vehicle product, adaptivity might not be required. However, when looking at the gradient of the signals, another conclusion can be drawn. Since the compensated radius is meant to be used for estimating tread wear over time. It cannot have a gradient equal to or greater than zero. For the FL tire on Test Case 4 the *Multiple Training* model has a similar slope to the adaptive model; meaning that it is acceptable, see Figure 6.1. However, on the rear tire the gradient is zero, see Figure 6.2. When analyzing the results on all tires on all available test cases, it is clear that the nonadaptive method gives unreliable performance. For Test Case 1 it seems to work fairly well on all tires. However, on Test Case 4 and Test Case 2 it gets a zero gradient on the rear tires and on Test Case 3 it gives unsatisfactory results on all tires, see Appendix, Figure 10.1-10.4. This behavior might not be acceptable in a final product. Meaning that this nonadaptive model, trained on several vehicle's does not work when looking at a larger scope.

7 | Adaptivity over Time

This chapter will investigate the possibility to have a time adaptive compensation model. That is a compensation model that changes its compensation parameters over time. It will present the method used to determine the time varying compensation factors, the results of the investigation and finally a discussion.

From Chapter 5 it is clear that the rolling radius depends on velocity, tire pressure and tire temperature. Chapter 6 clarifies that these dependencies changes between different tires and that the compensation factors that worked on one tire set does not necessarily work on another set, meaning that a compensation model needs to adapt to the current tires. One question that remains is the need for adaptivity over time. That is, does the effective rolling radius dependency on external factors change over time? Due to time limitations in the final stage of the thesis, this investigation was limited to only focus on the velocity dependency factor, k_v.

7.1 Method

Adaptivity over time was investigated on the *Linear* compensation model in (5.4) and (5.5). Unlike in Chapter 5 where the linear regression was performed on the entire data set, and the corresponding dependency factors (k_v, k_p, k_T, k_{TD}) were constant over time, the model in this chapter has compensation factors that vary with time. However, it was quickly discovered that, since the linear regression model in (5.4) has 5 degrees of freedom. 5 degrees of freedom means that there are many solutions that result in a similar final regression model. For example, the tire temperature and tire pressure has a large correlation, meaning that k_T could decrease while k_p could increase between iterations; and the outcome would be the same. Meaning that if one were to analyze the k_p over time, the variation could just be explained by the consequent change in k_T or any other degree of freedom, and not that the actual tire pressure dependency has changed. To minimizes the effect of this, only one degree of freedom was allowed to vary over time. In this thesis only the k_v factor was allowed to vary over time.

The regression model is on the form

$$\hat{r}_{V-Adaptive}(t) = k_v(t) \cdot v(t) + k_{p,1} \cdot p(t) + k_{T,1} \cdot T(t) + k_{TD,1} \cdot l_{TD}(t) + m_1, \tag{7.1}$$

where $\hat{r}_{V-Adaptive}(t)$ is the time dependent linear regression model. The subscript 1 indicates the parameters are constant over time and $k_v(t)$ is the time dependent velocity dependency factor. The corresponding compensation model is called *V-Adaptive* and is defined as

$$r_{comp,V-Adaptive} = r_{pc}(t) - k_v(t) \cdot v(t) - k_{p,1} \cdot p(t) - k_{T,1} \cdot T(t), \tag{7.2}$$

where $r_{comp,V-Adaptive}$ is the compensated rolling radius. The compensation factor was calculated by first determining the time-independent factors ($k_{p,1}, k_{T,1}, k_{TD,1}$ and m_1). This was calculated using linear least squares over the entire data set with the model in (5.4). The time dependent compensation factor, k_v was calculated by applying linear least squares regression over a "sliding window". I.e., the dependency factor is calculated for shorter segments of the entire test case (window) and then the window slides and the factor are recalculated. The window was in this case 100,000 s long and for each iteration the window slides 100 s.

The performance of the compensation was evaluated by training the model on the entire data set; and then applying the compensation model to the same data set and calculating standard deviations as

described in Section 5.1.7. This means that the *V-Adaptive* model was self-validated. K-fold validation cannot be used in this case since k_v varies with time, and if one do not validate on the same data points as the model has been trained on; the k_v for the validation data is unknown.

7.2 Result

This section presents the results of the adaptivity over time investigation.

Figure 7.1-7.4 presents the results of the time adaptive investigation. These plots include the compensated rolling radius, $r_{comp,V-Adaptive}$, that has been compensated using (7.2). The standard deviation for all four test cases are presented in Table 7.1-7.4. These tables shows the standard deviation of the pre-compensated rolling radius signal, the standard deviation of the compensated rolling radius when using the *Linear* method (that has time-constant compensation factors) and also the standard deviation of the *V-Adaptive* compensation method. Overall, in 14 out of the total 16 tires in the available data set, the *V-Adaptive* model performs better than the *Linear* model.

Table 7.1: This table shows the standard deviation for four different compensation methods for Test Case 1.

Compensation Method	FL	FR	RL	RR
Pre-compensated	0.287	0.279	0.328	0.307
Linear	0.077	0.071	0.111	0.085
V-Adaptive	0.076	0.077	0.111	0.087

Table 7.2: This table shows the standard deviation for four different compensation methods for Test Case 2.

Compensation Method	FL	FR	RL	RR
Pre-compensated	0.313	0.313	0.341	0.323
Linear	0.074	0.082	0.085	0.095
V-Adaptive	0.068	0.080	0.085	0.095

Table 7.3: This table shows the standard deviation for four different compensation methods for Test Case 3.

Compensation Method	FL	FR	RL	RR
Pre-compensated	0.256	0.246	0.308	0.305
Linear	0.112	0.108	0.126	0.124
V-Adaptive	0.104	0.100	0.116	0.110

Table 7.4: This table shows the standard deviation for four different compensation methods for Test Case 4.

Compensation Method	FL	FR	RL	RR
Pre-compensated	0.168	0.157	0.202	0.188
Linear	0.053	0.060	0.083	0.086
V-Adaptive	0.042	0.048	0.073	0.074

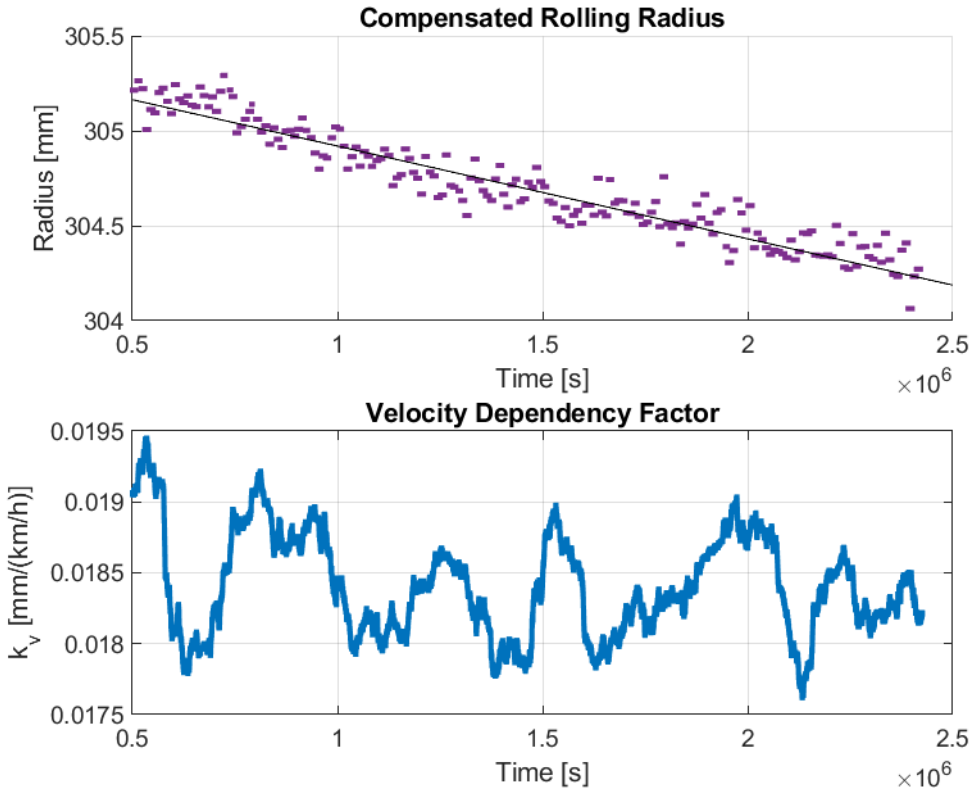

Figure 7.1: This figure shows the compensated rolling radius and the velocity dependency factor, k_v. This is for the FL tire on Test Case 1.

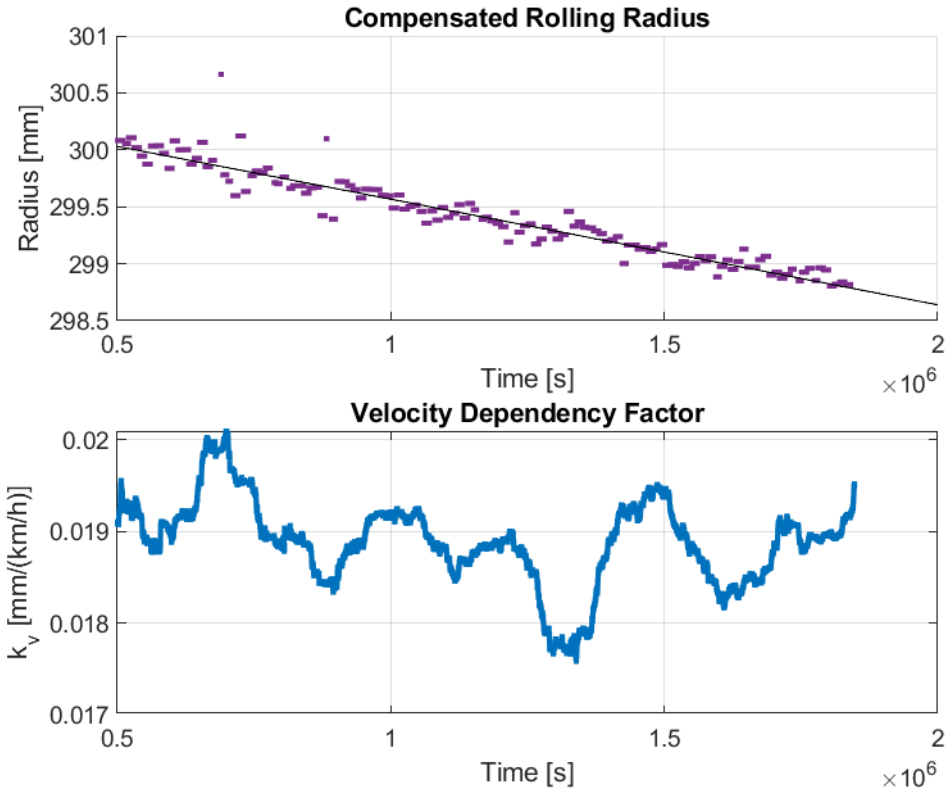

Figure 7.2: This figure shows the compensated rolling radius and the velocity dependency factor, k_v. This is for the FL tire on Test Case 2.

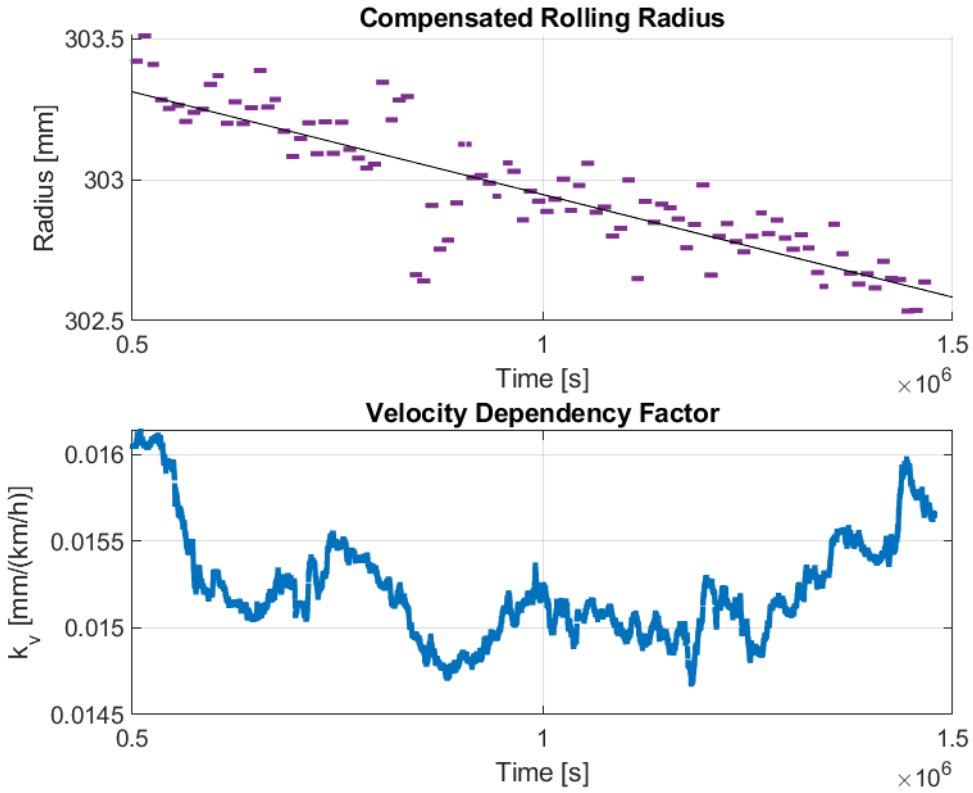

Figure 7.3: This figure shows the compensated rolling radius and the velocity dependency factor, k_v. This is for the FL tire on Test Case 3.

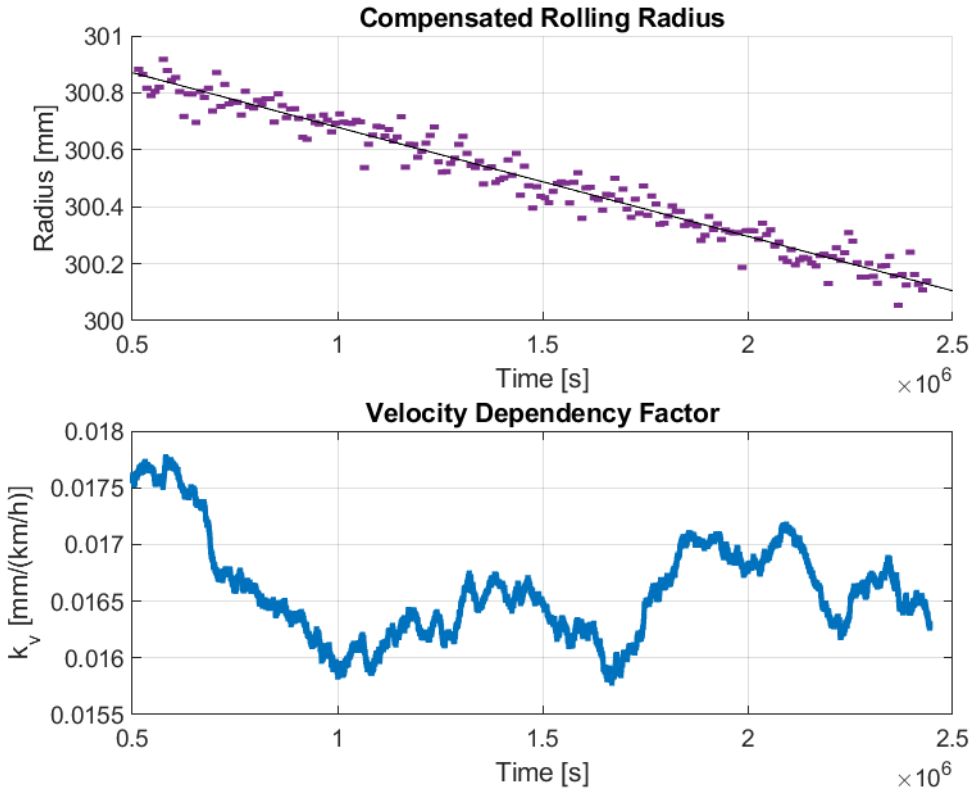

Figure 7.4: This figure shows the compensated rolling radius and the velocity dependency factor, k_v. This is for the FL tire on Test Case 4.

7.3 Discussion

This section presents the discussion of the adaptivity over time investigation.

The results showed that in 14 out of 16 cases of the available data set the *V-Adaptive* model performed better than the *Linear* model. The performance gains in terms of decrease in standard deviation, between the *V-Adaptive* model and the *Linear* model, was at most 20%. The results presented in this chapter were based on self-validation. Self-validation cannot be used to reliably evaluate the performance of a model. This means that the 20% performance gains does not mean that the *V-Adaptive* model is actually 20% better than the *Linear* model. Since the *V-Adaptive* model changes the k_v value over time it has a greater ability to adapt to the data than the *Linear* model. This means that when self-validating, the *V-Adaptive* model should always perform better than the *Linear* model since it can overfit the data more.

The reason for only 14 out of 16 cases having a lower standard deviation, when the *V-adaptive* model in theory always should be better, could be an effect of using the sliding window method. This is because the sliding window uses least squares on the data samples 100,000 s before the current time point. The first k_v value is calculated at time step t = 500,000 s. This means that k_v at time step 500,000 s is calculated using least squares on the time interval 400,000-500,000 s. This time interval includes tire growth. This could cause the least squares to calculate a k_v that is somewhat distorted. It is not until time step t = 600,000 s that no data samples including tire growth are used. Furthermore, another reason for this could be that the k_v values are calculated using the sliding window of 100,000 data samples, meaning that each k_v value is determined by using the last 100,000 data samples instead of only using the "new" 100 data samples. This means that the k_v that is applied to each 100 s segment is not the optimal solution for that time interval but the time interval for all 100,000 s before. This is an effect of using the sliding window. An alternate approach would be to use batches instead of a sliding

window. This does however have issues with large discrete jumps in the values of k_v. And if one wanted the same time step using batches as the sliding window used here, one would need batches of 100 s. This would be very sensitive to noise.

However, since the performance gains of the *V-Adaptive* model was not significantly better than the *Linear* model, it seems to indicate that the actual time dependency might not be that important. So, a final in-vehicle model might not need to take this into account. Further investigations are necessary to draw any clear conclusions.

When investigating the behavior of the velocity dependency factor, k_v, over time in Figure 7.1-7.4 one can observe how this factor has clear plateaus over longer time spans. I.e., levels of a almost constant k_v value. If considering Figure 7.4 at around time $1.7 \cdot 10^6$ s there is a clear increase in k_v value after being quite constant over a long time. In general, there are quite large variations in k_v value which could be an indication that other external factors that haven't been considered in the compensations does impact the value of k_v or that the compensations needs to be more precise to avoid these variations. Since the vehicles investigated in this thesis has exclusively been taxi cars, one possible reason for this behavior could be the constantly changing load and load distribution of the vehicles due to the number of passenger and luggage.

Overall, there seems to be no clear trends over time in the k_v parameter. Over time the tire is affected by overall health degradation and tread wear. Since there is no trend in how k_v varies over time (no steady decline or incline), this would indicate that there is no relationship between tire health degradation or tread wear and k_v. This is in a sense positive for a final, in-vehicle product. Since this would mean that it does not need to take into account how it varies with time. Meaning that if it were to try to estimate k_v online, it could use all additional data it gets to get a more accurate estimate of k_v instead of needing to recalculate k_v as it varies with time. It will however still be a challenge to get a good early estimate of k_v online, since even though the model can assume that it is constant over time; the "true" k_v could vary up and down making it difficult to get a good, time-independent estimate of k_v.

8 | Conclusion

In this thesis the possibility to develop an adaptive rolling radius compensation model has been investigated. The purpose of the investigation was to find methods that could be useful in a final, in-vehicle rolling radius estimation model. Different models have been developed and tested with the purpose of determining if rolling radius estimation can be done using sensor fusion, if rolling radius compensation is possible and if adaptive compensation is necessary.

Concerning the rolling radius estimation using sensor fusion. It was found in this thesis that the quality of the sensors, and their corresponding signals is essential to get a successful rolling radius estimate. For the data available for this thesis, it was found that the lack of three axes of the IMU, caused the method to be futile. This answers **RQ1**: "Can a tire's rolling radius estimation be improved by estimating the velocity using sensor fusion?". The thesis have shown that, given the available data set, it is not possible to get a rolling radius estimate better than the initial, raw rolling radius signal, using sensor fusion of the GPS and IMU data. For vehicle's with IMU:s that have all 6 axes, this method could be possible. This was however, not possible to investigate in this thesis.

Regarding the possibility to compensate the rolling radius signal. This thesis has presented a model that successfully compensates the rolling radius and significantly reduces signal noise. The best model found in this thesis was the *V-Quadratic* model, that compensates using linear tire temperature and tire pressure factors and quadratic velocity factors. After compensation, medians have been applied in segments of 10,000 s, to reduce measurement noise. It has been proven on Test Case 3 that the model can compensate for large pressure drops. This answers **RQ2**: "How can the effective rolling radius of a tire be compensated with respect to external factors?". Yes, a tire's rolling radius can be compensated with respect to tire pressure, tire temperature and vehicle velocity. The model developed is a so called offline model, meaning that it has knowledge of certain aspects that would not be possible in an online, in-vehicle model. This knowledge have been used to get the best possible model. This means that the model and method presented in this thesis are not applicable to a real life in-vehicle model. The reason for this is that the thesis aims to investigate if it possible to compensate a model; not to find how to do it online.

Considering the need for adaptive compensation. Due to the varying results between the different test cases, it was found that it is necessary to ensure the quality of the compensation. This thesis has covered several approaches to investigate the need of adaptive compensation factors between different vehicles and tire combinations. It was found that, depending on the requirements on the final in-vehicle product, a non-adaptive approach yield satisfactory values when looking at the noise reduction between different vehicles and tire set as long as no major abnormality (such as big pressure drops) is present. However, in the real world this is almost inevitable. When looking at the gradient of the rolling radius signal for the different vehicles, the approach of using a non-adaptive model is very inconsistent and often results in a compensated rolling radius with zero slope, i.e., no effects of tread wear. This answers **RQ3**: "Is there a need for adaptive compensation factors between different tire sets?". Yes, adaptive compensation factors between different tire sets is necessary.

Regarding the investigation considering adaptivity over time it was found that a final in-vehicle tread wear estimation model does not need to take this into account. However, further investigations are necessary to draw any clear conclusions on how the factors depend on time.

9 Further Work

To make it possible to implement the rolling radius compensation in an actual product there is a need of making the compensation work online. Online means that it needs to be able to operate in a vehicle while driving, and applying the compensation as it goes. The conversion to a online solution would bring some additional limitations. The current, offline solution, only investigates the possibility to compensate the effective rolling radius when having access to the entire data set. In an online compensation model, the compensations needs to be applied as the measurements are performed. This means that an online model has no knowledge of future data points, meaning that it needs to adapt the compensation model to the available data thus far. In the early stages of the tires' life cycle this means that there will be only a few data points available. In-vehicle system typically has limitations on memory and storage, meaning that the model can only store a certain amount of data points. The model presented in this thesis calculates the compensation factors using millions of data points at a time. In an online model this would need to be reduced by several orders of magnitude. An additional complication is the fact that the model in this thesis uses measured tread wear, this is not possible in an online model. The reason for including measured tread wear is to avoid overcompensation. An alternate approach could be to include the time variable in the model. Some test cases in this thesis has only two tread measurements which has then been interpolated to achieve a continuous signal. This interpolation means that it decreases linearly with time. In this case; a model that assumes linear time dependence would perform exactly the same, since the tread wear signal also decreases linearly with time. Furthermore, to be able to implement the tread wear estimation a translation from rolling radius to tread wear is needed.

Regarding the compensation factors, as mentioned in Chapter 1.4, this thesis only consider the velocity, tire pressure and tire temperature compensation. Other compensation factors, such as slip, yaw rate and load could also be investigated. Load compensation could be performed by using axle height sensors. Regarding the load compensation, the main reason why this isn't investigated in this thesis is due to the available data base, none of the existing test cases had both the dTPMS and the axle height sensors. One possible solution to this could be to include an independent investigation over the load compensation without using the compensations for the velocity, tire pressure and tire temperature. Additionally, a further investigation regarding the adaptivity between tire sets would be to evaluate the performance of these dependency factors between different test cases of the same vehicle model with the same tire model. If the same compensation model performs equally well on different test cases with the same vehicle and tire model, a final in-vehicle compensation model could use predefined compensation factors assuming that it knows which tire it has at a given time. This was not covered in this thesis due to limiting available data.

The method for rolling radius estimation in Chapter 4 did not work as intended. The reason for this was the specifications of the IMU. If one had access to a data base including vehicles with higher quality IMU:s this method might be fruitful. However, the model would need to be changed to estimate the vehicle's pitch angle and the ground's slope, and then compensate the IMU signals for these signals.

In this thesis the tire growth phenomenon was handled by simply skipping that part of the tire set cycle. This was done by skipping the first 0.5 million seconds of the test case. The 0.5 million was chosen by investigating Test Case 4. In reality the growth phenomenon might have different duration on different vehicles or tires. Also if one puts on slightly used tires, then one does not need to adjust for the tire growth. A final product needs to be able to detect the tire growth and compensate for it for the individual tire set.

Resolution of the tire pressure signal was a problem, previously mentioned in Chapter 5.1.2. If having a pressure sensor with the desired resolution from the beginning would facilitate the work and yield a more accurate tire pressure signal than the one which is currently modelled using the tire temperature signal. Finally, this thesis have only considered summer tires and passenger cars, it would therefore be interesting to examine the results on studded/friction tires and on different types of vehicles, such as trucks, buses and motorcycles.

Regarding the need for adaptivity over time. It was found in this thesis that this might not be necessary for the velocity dependency factor k_v. Due to time limitations only k_v was investigated. Further work would need to investigate if k_p and k_T are dependent on time. This could however pose a difficulty, since the large correlation between tire pressure and tire temperature could make it difficult to determine if only the tire pressure dependency is time dependent, if only the tire temperature is time dependent or both. There is also a problem when letting several degrees of freedoms vary over time, as discussed in Section 7.1. How to handle this issue would also need additional investigations. Another issue with investigating if k_p and k_T vary with time, is that the least squares regression requires a certain amount of variation in the signal to get an accurate estimate of the relationship between variables. Over shorter time segments the tire temperature and especially the tire pressure can be rather stable, and given the low resolution of both signals, one might only get a few different discrete values of the signals. This can make the least squares regression perform really poor since it lacks the data necessary to find a relationship between the signals and rolling radius. This is not the case in the velocity signal, which vary a lot. This means that the method used to evaluate if k_v varies with time might not be applicable for k_p and k_T.

10 | Appendix

This chapter will include additional plots and tables.

Table 10.1: Standard deviations for *Linear*, *V-Quadratic* and *Quadratic* compensation models for each tire and validated on each data fold. The table also includes means of the standard deviation for each tire over all folds. The values are for Test Case 1.

Standard Deviations												
Fold	*Linear*				*V-Quadratic*				*Quadratic*			
	FL	FR	RL	RR	FL	FR	RL	RR	FL	FR	RL	RR
1	0.072	0.065	0.106	0.082	0.07	0.066	0.104	0.079	0.069	0.066	0.102	0.078
2	0.061	0.058	0.091	0.073	0.054	0.05	0.084	0.066	0.056	0.05	0.085	0.065
3	0.068	0.086	0.102	0.101	0.063	0.074	0.094	0.088	0.065	0.074	0.094	0.089
4	0.056	0.047	0.086	0.068	0.054	0.044	0.076	0.06	0.054	0.044	0.076	0.059
5	0.058	0.064	0.062	0.064	0.054	0.06	0.064	0.072	0.06	0.08	0.067	0.091
Mean	0.063	0.064	0.089	0.077	0.059	0.059	0.084	0.073	0.061	0.063	0.085	0.076

Table 10.2: Standard deviations for *Linear*, *V-Quadratic* and *Quadratic* compensation models for each tire and validated on each data fold. The table also includes means of the standard deviation for each tire over all folds. The values are for Test Case 2.

Standard Deviations												
Fold	*Linear*				*V-Quadratic*				*Quadratic*			
	FL	FR	RL	RR	FL	FR	RL	RR	FL	FR	RL	RR
1	0.097	0.114	0.104	0.117	0.074	0.092	0.088	0.102	0.071	0.091	0.082	0.095
2	0.05	0.057	0.062	0.071	0.044	0.06	0.055	0.073	0.048	0.062	0.057	0.072
3	0.064	0.073	0.077	0.079	0.053	0.069	0.071	0.081	0.061	0.068	0.067	0.077
4	0.063	0.067	0.068	0.075	0.058	0.063	0.067	0.075	0.089	0.087	0.068	0.076
5	0.057	0.068	0.094	0.105	0.07	0.069	0.075	0.087	0.066	0.068	0.074	0.086
Mean	0.066	0.076	0.081	0.089	0.06	0.071	0.071	0.084	0.067	0.075	0.069	0.081

Table 10.3: Standard deviations for *Linear*, *V-Quadratic* and *Quadratic* compensation models for each tire and validated on each data fold. The table also includes means of the standard deviation for each tire over all folds. The values are for Test Case 3.

Standard Deviations												
Fold	*Linear*				*V-Quadratic*				*Quadratic*			
	FL	FR	RL	RR	FL	FR	RL	RR	FL	FR	RL	RR
1	0.056	0.065	0.05	0.056	0.062	0.072	0.054	0.066	0.057	0.066	0.051	0.07
2	0.08	0.079	0.095	0.109	0.072	0.075	0.091	0.113	0.085	0.084	0.095	0.11
3	0.181	0.162	0.21	0.183	0.177	0.159	0.207	0.178	0.177	0.159	0.204	0.178
4	0.074	0.084	0.069	0.081	0.069	0.082	0.074	0.086	0.067	0.075	0.072	0.078
5	0.04	0.037	0.053	0.059	0.036	0.033	0.046	0.043	0.043	0.045	0.071	0.085
Mean	0.086	0.085	0.095	0.098	0.083	0.084	0.094	0.097	0.086	0.086	0.098	0.104

Table 10.4: Standard deviations for *Linear*, *V-Quadratic* and *Quadratic* compensation models for each tire and validated on each data fold. The table also includes means of the standard deviation for each tire over all folds. The values are for Test Case 4.

Standard Deviations												
Fold	*Linear*				*V-Quadratic*				*Quadratic*			
	FL	FR	RL	RR	FL	FR	RL	RR	FL	FR	RL	RR
1	0.045	0.057	0.072	0.087	0.044	0.056	0.068	0.085	0.043	0.058	0.066	0.082
2	0.043	0.046	0.056	0.063	0.044	0.047	0.056	0.063	0.042	0.043	0.051	0.061
3	0.041	0.052	0.068	0.069	0.04	0.054	0.067	0.071	0.044	0.052	0.071	0.074
4	0.038	0.047	0.063	0.056	0.036	0.042	0.068	0.06	0.036	0.046	0.068	0.058
5	0.045	0.04	0.087	0.073	0.054	0.045	0.092	0.075	0.054	0.048	0.091	0.076
Mean	0.042	0.048	0.069	0.069	0.043	0.049	0.07	0.071	0.044	0.049	0.069	0.07

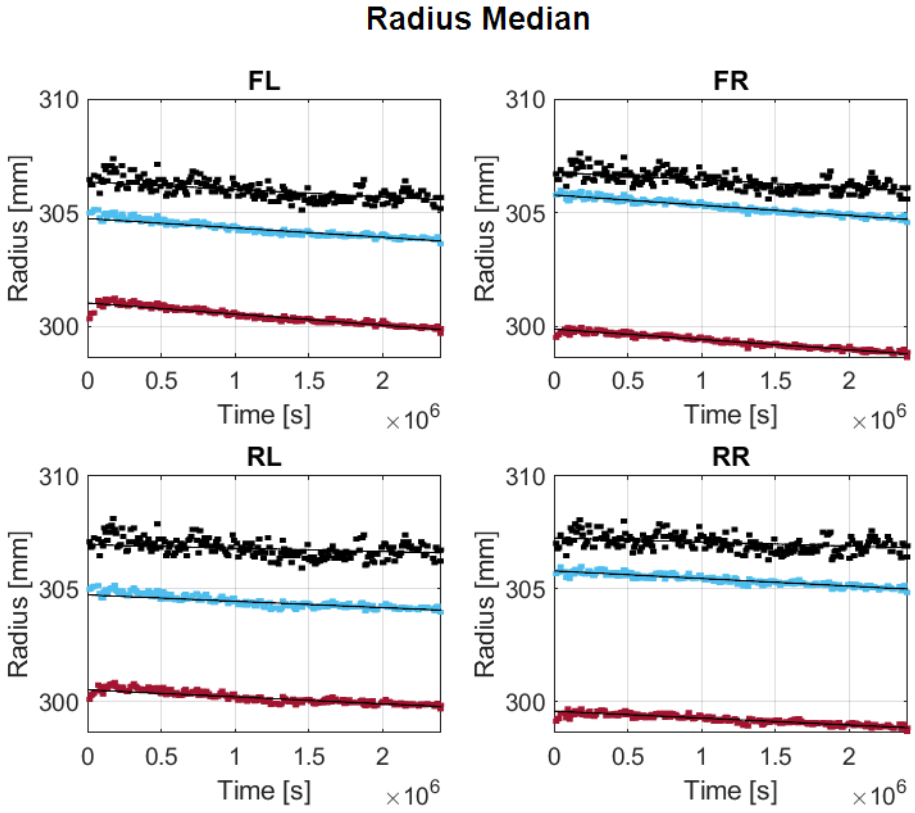

Figure 10.1: This figure illustrates the pre-compensated radius signal in black, the V-Quadratic compensation in red and the *Multiple Training* in blue. All tires on Test Case 1.

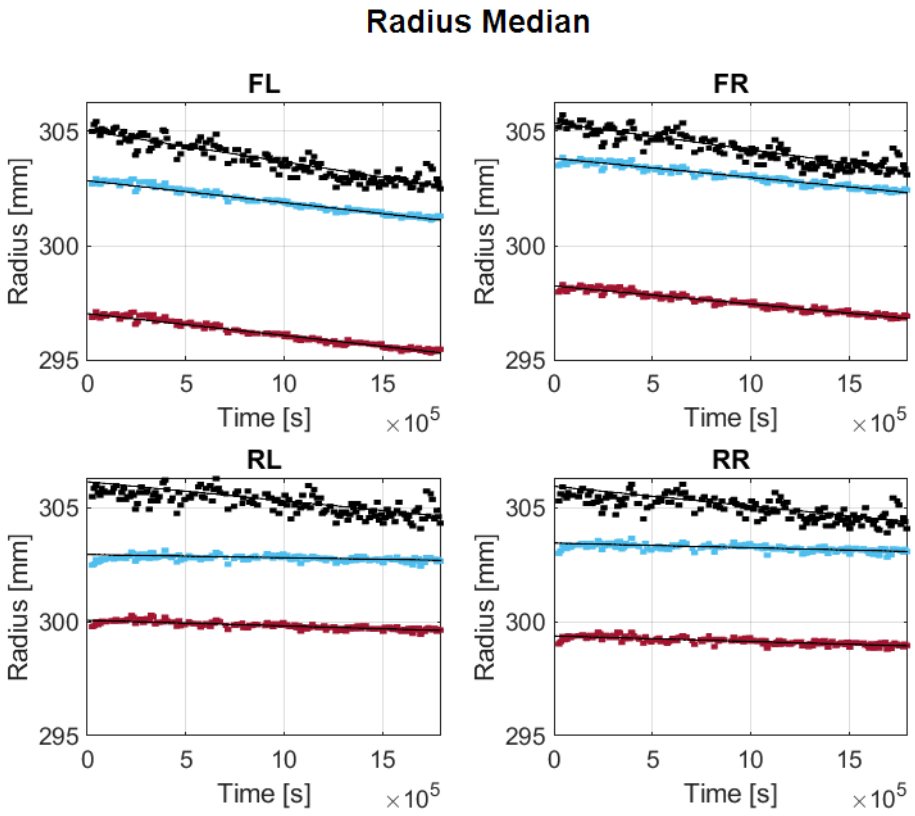

Figure 10.2: This figure illustrates the pre-compensated radius signal in black, the V-Quadratic compensation in red and the *Multiple Training* in blue. All tires on Test Case 2.

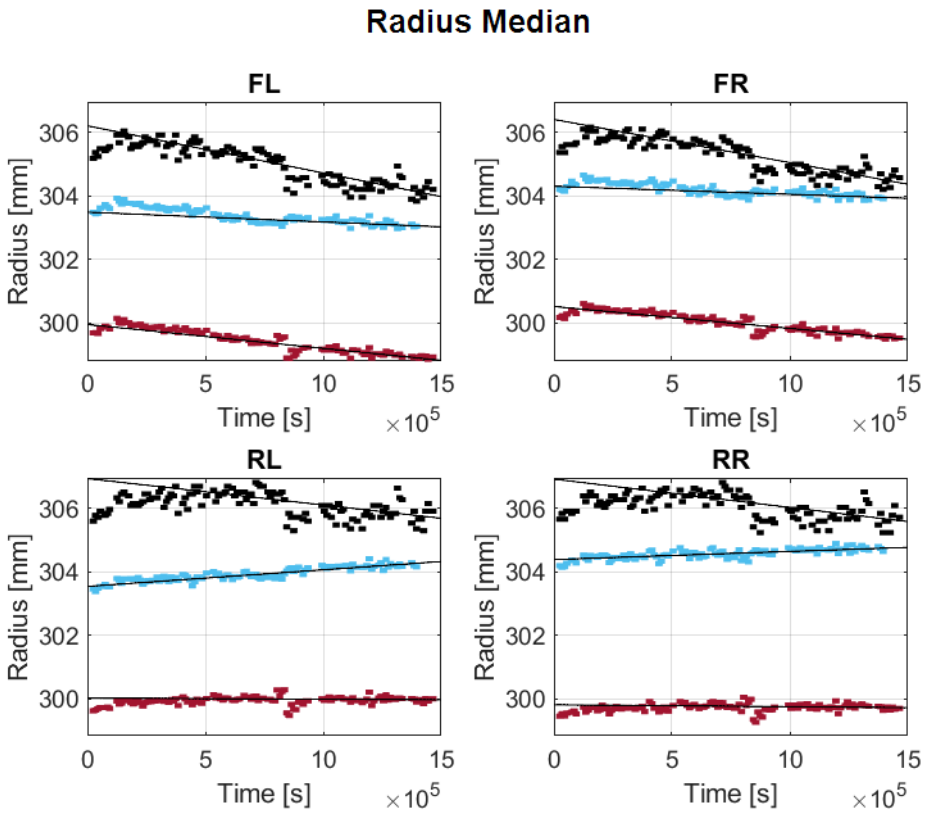

Figure 10.3: This figure illustrates the pre-compensated radius signal in black, the V-Quadratic compensation in red and the *Multiple Training* in blue. All tires on Test Case 3.

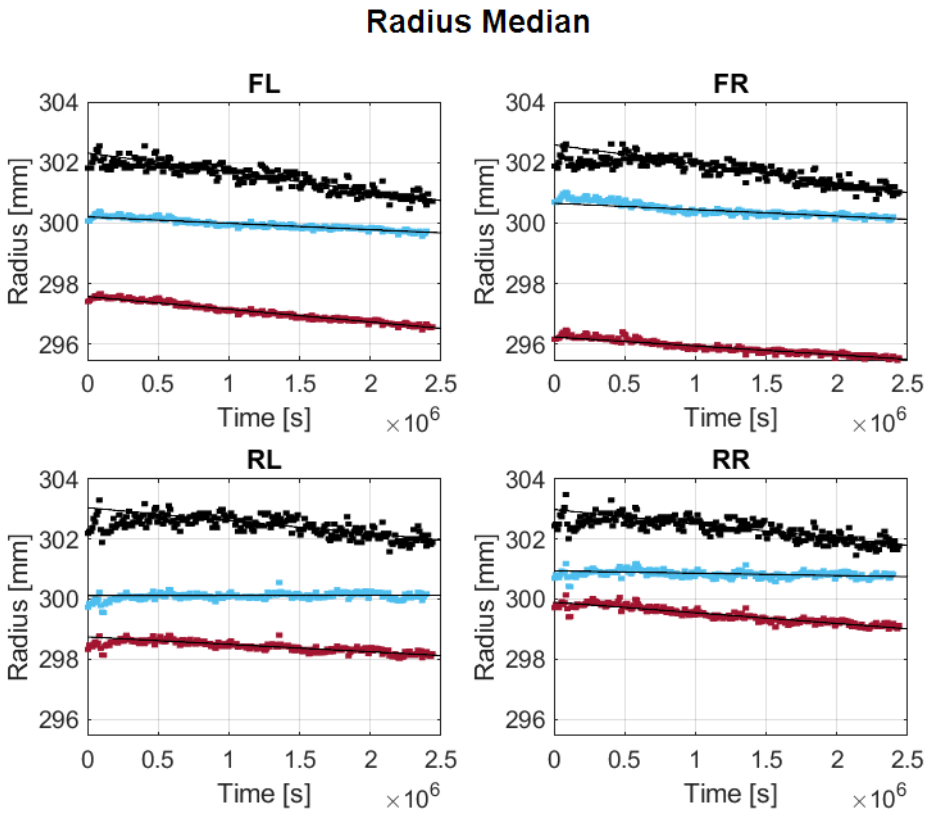

Figure 10.4: This figure illustrates the pre-compensated radius signal in black, the V-Quadratic compensation in red and the *Multiple Training* in blue. All tires on Test Case 4.

Bibliography

[1] J. Y. Wong, *Theory of Ground Vehicles*, 4th ed. Hoboken, New Jersey: John Wiley Sons, Inc, 2008.

[2] E. Choi *et al.*, "Tire-related factors in the pre-crash phase," *Report No. DOT HS*, vol. 811, p. 617, 2012.

[3] B. Allbert, "Tires and hydroplaning," *SAE Transactions*, pp. 593–603, 1968.

[4] R. Dumas, *Council directive of 18 july 1989 on the approximation of the laws of the member states relating to the tread depth of tyres of certain categories of motor vehicles and their trailers*, 1989. [Online]. Available: `https://eur-lex.europa.eu/legal-content/EN/ALL/?uri=CELEX%5C%3A31989L0459`.

[5] Transportstyrelsen, *Däck*, 2022. [Online]. Available: `https://www.transportstyrelsen.se/sv/vagtrafik/fordon/fordonsregler/dack/`.

[6] S. W. Lee, K. M. Jeong, K. W. Kim, J. H. Kim, *et al.*, "Numerical estimation of the uneven wear of passenger car tires," *World Journal of Engineering and Technology*, vol. 6, no. 04, p. 780, 2018.

[7] G. Genta, *Motor Vehicle Dynamics - Modeling and Simulation*. Singapore: World Scientific, 1997, vol. 43.

[8] K. Kim, H. Park, and T. Kim, "Comparison of performance of predicting the wear amount of tire tread depending on sensing information," *Sensors*, vol. 23, no. 1, p. 459, 2023.

[9] M. He and X. Lin, "Connected tyres: Real-time tyre monitoring system for fleet& autonomous vehicles with tyre wearestimation through sensor fusion," M.S. thesis, 2020.

[10] H. S. Ga and J. Y. Kang, "Tire dynamic rolling radius compensation algorithm based on ax sensor offset estimation for i-tpms," *International Journal of Automotive Technology*, vol. 22, no. 6, pp. 1579–1587, 2021.

[11] T. Poloni and J. Lu, "An indirect tire health monitoring system using on-board motion sensors," SAE Technical Paper, Tech. Rep., 2017.

[12] Y. Wei, C. Oertel, X. Li, and L. Yu, "A theoretical model for the tread slip and the effective rolling radius of the tyres in free rolling," *Proceedings of the Institution of Mechanical Engineers, Part D: Journal of Automobile Engineering*, vol. 231, no. 11, pp. 1461–1470, 2017.

[13] T. Glad and L. Ljung, *Reglerteknik - Grundläggande teori*, 4th ed. Lund: Studentlitteratur, 2006.

[14] T. Glad and L. Ljung, *Reglerteori - Flervariabla och olinjära metoder.* 2nd ed. Lund: Studentlitteratur, 2003.

[15] M. N. Mahyuddin, J. Na, G. Herrmann, X. Ren, and P. Barber, "Adaptive observer-based parameter estimation with application to road gradient and vehicle mass estimation," *IEEE Transactions on Industrial Electronics*, vol. 61, no. 6, pp. 2851–2863, 2013.

[16] R. E. Kalman, "A new approach to linear filtering and prediction problems," 1960.

[17] J. Dakhlallah, S. Glaser, S. Mammar, and Y. Sebsadji, "Tire-road forces estimation using extended kalman filter and sideslip angle evaluation," in *2008 American control conference*, IEEE, 2008, pp. 4597–4602.

[18] N. Persson, F. Gustafsson, and M. Drevö, "Indirect tire pressure monitoring using sensor fusion," *SAE Transactions*, pp. 1657–1662, 2002.

[19] F. Gustafsson, *Statistical Sensor Fusion.* 2nd ed. Lund: Studentlitteratur, 2012.

[20] K. Dunn, "Process improvement using data, 2010," *Available through download at https://learnche. org/pid/PID. pdf*, pp. 157–174, 2023.

[21] L. Xiong, X. Xia, Y. Lu, W. Liu, L. Gao, S. Song, Y. Han, and Z. Yu, "Imu-based automated vehicle slip angle and attitude estimation aided by vehicle dynamics," *Sensors*, vol. 19, no. 8, p. 1930, 2019.